PB 161553

NBS

# Technical Note No. 52

Boulder Laboratories

# FIELD STRENGTH CALCULATIONS FOR E.L.F. RADIO WAVES

BY JAMES R. WAIT AND NANCY F. CARTER

U. S. DEPARTMENT OF COMMERCE
NATIONAL BUREAU OF STANDARDS

## THE NATIONAL BUREAU OF STANDARDS

### Functions and Activities

The functions of the National Bureau of Standards are set forth in the Act of Congress, March 3, 1901, as amended by Congress in Public Law 619, 1950. These include the development and maintenance of the national standards of measurement and the provision of means and methods for making measurements consistent with these standards; the determination of physical constants and properties of materials; the development of methods and instruments for testing materials, devices, and structures; advisory services to government agencies on scientific and technical problems; invention and development of devices to serve special needs of the Government; and the development of standard practices, codes, and specifications. The work includes basic and applied research, development, engineering, instrumentation, testing, evaluation, calibration services, and various consultation and information services. Research projects are also performed for other government agencies when the work relates to and supplements the basic program of the Bureau or when the Bureau's unique competence is required. The scope of activities is suggested by the listing of divisions and sections on the inside of the back cover.

### Publications

The results of the Bureau's work take the form of either actual equipment and devices or published papers. These papers appear either in the Bureau's own series of publications or in the journals of professional and scientific societies. The Bureau itself publishes three periodicals available from the Government Printing Office: The Journal of Research, published in four separate sections, presents complete scientific and technical papers; the Technical News Bulletin presents summary and preliminary reports on work in progress; and Basic Radio Propagation Predictions provides data for determining the best frequencies to use for radio communications throughout the world. There are also five series of nonperiodical publications: Monographs, Applied Mathematics Series, Handbooks, Miscellaneous Publications, and Technical Notes.

Information on the Bureau's publications can be found in NBS Circular 460, Publications of the National Bureau of Standards ($1.25) and its Supplement ($1.50), available from the Superintendent of Documents, Government Printing Office, Washington 25, D.C.

NATIONAL BUREAU OF STANDARDS
*Technical Note*
52

March 1960

# FIELD STRENGTH CALCULATIONS FOR E. L. F. RADIO WAVES

by

James R. Wait and Nancy F. Carter

NBS Technical Notes are designed to supplement the Bureau's regular publications program. They provide a means for making available scientific data that are of transient or limited interest. Technical Notes may be listed or referred to in the open literature. They are for sale by the Office of Technical Services, U. S. Department of Commerce, Washington 25, D. C.

DISTRIBUTED BY

UNITED STATES DEPARTMENT OF COMMERCE

OFFICE OF TECHNICAL SERVICES

WASHINGTON 25, D. C.

Price $ .50

# TABLE OF CONTENTS

# FIELD STRENGTH CALCULATIONS FOR E. L. F. RADIO WAVES


## Abstract

The mode theory of propagation of electromagnetic waves at extremely low frequencies (1.0 to 3000 c/s) is briefly reviewed in this paper. Starting with the representation of the field as a sum of modes, approximate formulas are presented for the attenuation and phase constants. At the shorter distances, where the range is comparable to the wavelength, the spherical-earth mode series is best transformed to a series involving cylindrical wave functions. This latter form is used to evaluate the near field behavior of the various field components. The effect of the earth's magnetic field is also evaluated using a quasi-longitudinal approximation which is particularly appropriate for propagation in the magnetic meridian. In general it is indicated that if the gyro frequency is comparable or greater than the effective value of the collision frequency, the presence of the earth's magnetic field may be important for E. L. F. In this case the attenuation may be increased somewhat. The influence of a purely transverse magnetic field is also considered.

This technical note is actually a numerical supplement to the paper "Mode Theory and the Propagation of ELF Radio Waves," by J.R. Wait, J. Research N.B.S., 64D, .... July/Aug. 1960; however, for sake of completeness the relevant theory is briefly presented.


## 1. Introduction

The propagation of electromagnetic waves at extremely low frequencies (E. L. F.) has received considerable attention recently [1-5]. Unfortunately, the experimental data in this frequency range (1.0 c/s to 3000 c/s) is still rather limited [8-15]. There is little doubt, however, that the bulk of the energy is transferred via a waveguide mode. The bounding surfaces of this waveguide are the ground and the lower edge of the ionospheric E region.

An important feature of E. L. F. propagation is that the distance between source and observer may be comparable to the wavelength. For example, at 300 c/s the wavelength is 1000 km. In fact, many of the experiments are carried out at distances of this order and account must be taken of the near field effects.

It is the purpose of this note to present computations based on the mode theory as it applies to E. L. F. propagation. It is also hoped that these results will also be of assistance in interpretation of future experimental data.

## II. Basic Theoretical Model

The assumed theoretical model is taken to be a homogeneous conducting spherical earth of radius a surrounded by a concentric conducting ionospheric shell of inner radius a + h. It is convenient to introduce the usual spherical coordinate system $(r, \theta, \phi)$. Using this model and assuming a vertical electric dipole source located at $\theta = 0$, $r = a$, the expression for the vertical electric field, $E_r$, is given by an expression of the following form [4, 16]

$$E_r = \frac{I\, ds\, \eta}{2kha^2} \sum_{n=0}^{\infty} \delta_n \frac{\nu(\nu+1)}{\sin \nu\pi} P_\nu(-\cos\theta) \tag{1}$$

where I - - average current in the source dipole;

ds - - length of source dipole;

$\eta$ - - intrinsic impedance of air space $\cong 120\pi$ ohms;

$P_\nu(-\cos\theta)$ - - Legendre function of argument $-\cos\theta$ and (complex) order $\nu$;

$\nu + \frac{1}{2} = ka\, S_n$ where $S_n$, for n = 0, 1, 2, . . . , determined from the boundary condition and is described below; and

$$\delta_n \cong \cfrac{1}{1 + \cfrac{\sin 2khC_n}{2khC_n}} \qquad \begin{aligned} &\cong 1/2 \text{ for } n = 0 \\ &\cong 1 \text{ for } n = 1, 2, 3 \ldots \end{aligned}$$

The individual terms in the above series correspond to the waveguide modes. In the general case, the factor $S_n$ is obtained from

the solution of a complicated transcendental equation which involves spherical Bessel functions of large argument and complex order. Certain aspects of this problem have been discussed by Schumann [1] and also the author [4]. For a homogeneous earth and a homogeneous ionosphere, both assumed isotropic, it has been shown that $S_n$ may be approximated by [17]

$$S_n = \left\{1 - \left(\frac{\pi n}{kh}\right)^2 \frac{1}{4}\left[1 + \sqrt{1 + 4i\,\frac{\Delta\, kh}{(\pi n)^2}}\,\right]^2\right\}^{\frac{1}{2}} \tag{2}$$

where $\Delta = \dfrac{1}{N_i} + \dfrac{1}{N_g}$

in terms of the refractive indices, $N_g$ and $N_i$, of the earth and the ionosphere, respectively. This equation is valid subject to the condition $|\Delta|\, kh << 1$. The sign of the radical is chosen in the above equation which makes the real part positive. The values of $S_n$ then are located in the fourth quadrant of the complex plane. When $n = 0$, the above simplifies to

$$S_o = \left[1 - i\,\frac{\Delta}{kh}\right]^{\frac{1}{2}} \cong 1 - i\,\frac{\Delta}{2\,kh} \tag{3}$$

Now, since $|\Delta|\, kh << 1$, the radical in equation (1) can be expanded for $n > 0$ to yield

$$S_n = \left[1 - \left(\frac{\pi n}{kh}\right)^2 - i\,\frac{2\Delta}{kh}\right]^{\frac{1}{2}} \text{ for } n = 1,\ 2,\ 3\ \ldots \tag{4}$$

Furthermore, if in addition,

$$\frac{|\Delta|}{kh} << 1 - \left(\frac{\pi n}{kh}\right)^2$$

it is permissible to write, for all n,

$$S_n \cong \left[1 - \left(\frac{\pi n}{kh}\right)^2\right]^{\frac{1}{2}} - i\,\frac{\epsilon_n}{2kh}\,\Delta\left[1 - \left(\frac{\pi n}{kh}\right)^2\right]^{-\frac{1}{2}} \tag{5}$$

where $\epsilon_o = 1$, $\epsilon_n = 2$ (for $n = 1,\ 2,\ 3\ \ldots$). This latter equation is valid when the "waveguide modes" are not near cut-off and is in the form given by Schumann [2]. It is quite analogous to the standard results for the propagation constant in a rectangular waveguide with finitely conducting walls [18, 19].

## III. Earth-Flattening Approximation

The possibility that the curvature of the earth may be neglected is now investigated. To simplify field calculations at relatively short distances, it would seem desirable to transform the mode series to a form where the first term corresponds to the model of a flat earth and the succeeding terms are corrections for curvature. This approach has been used by Pekeris [20] and more recently by Koo and Katzin [21] in their investigations of microwave duct propagation. From their work, it may be shown that

$$\frac{P_\nu(-\cos\theta)}{\sin\nu\pi} \cong H_0^{(2)}(kS_n\rho) - \frac{1}{12}\left(\frac{\rho}{a}\right)^2 H_2^{(2)}(kS_n\rho) \tag{6}$$

$$+ \text{ terms in } (\rho/a)^4,\ (\rho/a)^6, \text{ etc.},$$

where $\nu + 1/2 = kS_n\rho$ and $\rho = a\theta$. $H_0^{(2)}$ and $H_2^{(2)}$ are Hankel functions of the second kind of order zero and two, respectively. When the great circle distance $\rho$ is reasonably small compared to the earth's radius a, only the first term in the expansion need be retained.

For convenience in what follows, it is desirable to express the field components as a ratio to the quantity

$$E_0 = i\,(\eta/\lambda)\, I\, ds\, (e^{-ik\rho})/\rho, \quad (\eta \cong 120\pi);$$

$E_0$ is the radiation field of the source at a distance $\rho$ on a perfectly conducting ground. Thus, for both the source and the observer near the ground, it is not difficult to show that

$$E_z = W\,E_0$$

where $$W \cong -i\pi\frac{\rho}{h}\, e^{ik\rho}\sum_{n=0}^{\infty}\delta_n\, S_n^2\, H_0^{(2)}(kS_n\rho) \quad , \tag{7}$$

$$E_\rho = -S\,E_0$$

where $$S \cong \frac{\pi}{N_g}\,\frac{\rho}{h}\, e^{ik\rho}\sum_{n=0}^{\infty}\delta_n\, S_n\, H_1^{(2)}(kS_n\rho) \tag{8}$$

and $$H_\phi = -T\,E_0/\eta$$

where $$T \cong -\pi \frac{\rho}{h} e^{ik\rho} \sum_{n=o}^{\infty} \delta_n S_n H_1^{(2)} (kS_n\rho) = -N_g S \qquad (9)$$

where terms containing $(\rho/a)^2$, $(\rho/a)^4$ have been neglected.

When $k\rho >> 1$, corresponding to the "far-zone," the above expressions may be simplified since the Hankel functions may be replaced by the first term of their asymptotic expansion. This leads to the compact result

$$\begin{bmatrix} W \\ S \\ T \end{bmatrix} \cong \frac{(\rho/\lambda)^{\frac{1}{2}}}{(h/\lambda)} e^{i[\frac{2\pi\rho}{\lambda} - \frac{\pi}{4}]} \sum_{n=o}^{\infty} \delta_n \begin{bmatrix} S_n^{3/2} \\ -S_n^{\frac{1}{2}}/N_g \\ S_n^{\frac{1}{2}} \end{bmatrix} e^{-i2\pi S_n \rho/\lambda} \qquad (10)$$

which is valid for $\rho >> \lambda$. As expected, the ratio of W to T for a given mode is $S_n$ which for low order or grazing modes is of the order of unity. The ratio of S to T, quite generally, is $-1/N_g$ which is very small compared to unity; in fact, it vanishes for a perfectly conducting ground as it must.

The excitation by a horizontal electric dipole may be treated in a similar manner. A complete discussion of the theory is given elsewhere [17]. The expression for the vertical field $E_z$ of the horizontal dipole Ids which is located at the origin and oriented in direction $\phi = 0$ may be written in the form

$$E_z = S E_o \cos\phi \qquad (11)$$

where S and $E_o$ are defined above. By using the reciprocity theorem, this result can also be deduced directly from equation (9). Comparing the above formula for $E_z$ (for a horizontal dipole) with corresponding formula for $E_z$, for a vertical dipole, it may be easily shown that

$$\frac{E_z \text{ (for horizontal dipole)}}{E_z \text{ (for vertical dipole)}} \cong \frac{\cos\phi}{N_g}\left(1 - \frac{1}{N_g^2}\right)^{\frac{1}{2}} \cong \frac{\cos\phi}{N_g} \qquad (12)$$

being valid in the asymptotic or far zone. In terms of the ground

conductivity $\sigma_g$ and dielectric constant $\epsilon_g$,

$$\frac{1}{N_g} = \left( \frac{i \epsilon_0 \omega}{\sigma_g + i \epsilon_g \omega} \right)^{\frac{1}{2}} \cong \left( \frac{i \epsilon_0 \omega}{\sigma_g} \right)^{\frac{1}{2}} .$$

This is a small quantity.

The above formulas for W, S, and T are valid only if $\rho \ll a$. If the first curvature correction term is included, it is a simple matter to show, in the "far zone", that this amounts to multiplying the right-hand side by the factor

$$1 + \frac{1}{12} \left( \frac{\rho}{a} \right)^2 \text{ or } 1 + \frac{\theta^2}{12} .$$

Starting from the mode series for a spherical earth [17] and using the far field approximation for the Legendre function, it turns out that W, S, T have precisely the same form as in equation (10) except the factor $(\theta/\sin\theta)^{\frac{1}{2}}$ occurs in the right-hand side. Noting that

$$\left( \frac{\theta}{\sin\theta} \right)^{\frac{1}{2}} \cong 1 + \frac{\theta^2}{12} + \text{terms in } \theta^4, \ \theta^6 \text{ , etc.}$$

it is apparent to a second order that the derived curvature correction is the same as from the Hankel function series.

## IV. Distance and Frequency Dependence

Certain features of the mode series are best illustrated by a graphical plot of field strength vs. distance under various values of the parameters. Since $N_g \gg N_i$ it may be safely assumed for E.L.F. that $\Delta = 1/N_i$. Then on the assumption that the ionosphere is behaving like a conductor, it is possible to write

$$N_i = \left( 1 - i \frac{\omega_r}{\omega} \right)^{\frac{1}{2}} \tag{13}$$

where

$$\omega_r = \frac{\omega_0^{\,2}}{\nu} = \frac{(\text{plasma frequency})^2}{\text{collision frequency}} .$$

The above relation for $N_i$ is an approximation which is valid when the collision frequency $\nu$ between electrons and neutral ions is much less than the angular frequency $\omega$. Since $\nu$ is of the order of $10^7$ in the lower E region, this is certainly valid at E.L.F. The (angular) plasma frequency $\omega_o$ is given by

$$\omega_o^2 = \frac{e^2 N}{\epsilon_o m}$$

where N is the electron density, e and m are charge and mass of the electron, and $\epsilon_o$ is the dielectric constant of free space. $\omega_r$, which is proportional to the ratio $N/\nu$, is believed to be of the order of $10^5$ in the D layer or the lower region of the E layer. At least this appears to be the effective value deduced from V.L.F. observations for highly oblique incidence [23]. At E.L.F. it appears that the waves are reflected at higher levels in the ionosphere and the effective value of $\omega_r$ is somewhat larger, being possibly of the order of $10^6$.

It should be noted in passing that $\omega_r$ may be replaced by $\sigma_i/\epsilon_o$ where $\sigma_i$ is the effective conductivity of the ionosphere and $\epsilon_o$ is the dielectric constant of free space.

To indicate the variation of the field as a function of distance, the magnitude and phase of T and W are shown in Figs. 1a to 4c for a range of values of $\omega_r$ and h = 90 km. The curves denoted $\omega_r = \infty$ correspond to a perfectly conducting ionosphere. These are presented for purposes of comparison with the set for the more reasonable values of $\omega_r$. These are $2 \times 10^6$ and $5 \times 10^5$. Actually, $|T|$ and $|W|$ are both divided by the square root of the distance $\rho$ (in kilometers) and plotted since the curves become linear at larger distances. The slope of these linear parts of the curves is proportional to the attenuation rate (in db per 1000 km) as usually defined. It is seen immediately that at the shorter distances, the curves are no longer straight. This immediately indicates that considerable caution should be exercised in computing attenuation rates from spectral analyses of "sferics." For example, it is only

when the distance $\rho$ exceeds about one-sixth of a wavelength, is it permissible to assume that log $(|W|/\sqrt{\rho})$ or log $(|E_z| \times \sqrt{\rho})$ vary in a linear manner with distance $\rho$. Similarly, the phase of W(or $E_z$) varies in a linear manner only when the distance exceeds about one-half wavelength. Similar remarks apply to the magnetic field variations with distance.

To shed further light on the nature of the E. L. F. fields in the waveguide, the radial impedance of the wave is now considered. It is noted that

$$- \left. \frac{E_z}{\eta H_\phi} \right]_{z=0} = \frac{W}{T} \tag{14}$$

which is by definition the (normalized) impedance of the wave looking in the radial or $\rho$ direction. First it should be noted that for $k\rho >> 1$,

$$\frac{W}{T} \cong 1$$

and for $k\rho << 1$ and $\rho << h$,

$$\frac{W}{T} \cong \frac{1}{ik\rho} \quad .$$

For the intermediate and interesting range, $k\rho$ is comparable to unity and $\rho$ is somewhat greater than h. Using the numerical values of T and W mentioned above, the ratio $|W/T|$ and the phase (lag) defined by arg T - arg W are plotted in Figs. 5a to 6c and as a function of distance for various frequencies. As before, h = 90 km and the same range of $\omega_r$ values are chosen.

The impedance ratio W/T is independent of the frequency spectrum of the source provided, of course, it may be represented by an equivalent vertical electric dipole. In fact, this complex ratio could be easily calculated from the frequency spectra of the waveforms of the vertical electric field and the horizontal magnetic field of an atmospheric. The observed variation of magnitude or phase of W/T as a function of frequency should then provide a basis for distance measuring. Such a scheme, while admittedly crude, requires only one receiving station equipped with a vertical whip and a loop antenna.

At the very short distances where $\rho$ is of the order of the ionospheric reflecting height (i.e., 90 km), the mode series representation for the fields is very poorly convergent. However, alternate representations are available which converge very rapidly in this case [17]. For $\omega_r = \infty$, these are

$$T = \sum_{m=0}^{\infty} \epsilon_m \left(\frac{\rho}{r_m}\right)^2 \left(1 - \frac{i}{kr_m}\right) e^{-ik(r_m - \rho)} \tag{15}$$

and

$$W = \sum_{m=0}^{\infty} \epsilon_m \frac{\rho}{r_m} \left\{ \left[ \left(1 - \frac{1}{(kr_m)^2}\right) - \frac{i}{kr_m} \right] - \left(\frac{2mh}{r_m}\right)^2 \left[ \left(1 - \frac{3}{(kr_m)^2}\right) - \frac{3i}{kr_m} \right] \right\} e^{-ik(r_m - \rho)} \tag{16}$$

where $r_m = \left[\rho^2 + (2mh)^2\right]^{\frac{1}{2}}$, $\epsilon_0 = 1$, $\epsilon_m = 2\,(m \neq 0)$.

Individual terms in these series correspond to the contribution from images of the source dipole. These particular expressions are exact on the assumption of perfectly conducting planes. (i.e., $\omega_r = \infty$ and $\sigma_g = \infty$). It is known, however, from the mode calculations that at short distances (i.e., for $\rho < 100$ km), the numerical values of the functions T and W are only very slightly dependent on the finite value of $\omega_r$ and $\sigma_g$. Thus (15) and (16) are generally applicable.

To illustrate the nature of the fields at short ranges, the magnitude and phase of T and W are shown plotted in Figs. 7a to 8b. The solid curves correspond to equations (15) and (16) for h = 90 km. The dashed curves correspond to equations (15) and (16) when h = $\infty$; this is the same as taking only the first term in the series. At the very short ranges, it is seen that the solid and dashed curves merge together. Apparently in this region, the reflecting layer at 90 km can be ignored. At the greater ranges, the T and W functions both approach unity for the case of no reflecting layer (i.e., h = $\infty$).

Corrections for earth curvature resulting from diffraction would, of course, modify these dashed curves at ranges exceeding about 500 km. It may be concluded from the information plotted in Figs. 7 and 8 that only for extremely short ranges (i.e., less than about 30 km) is it permissible to neglect the presence of the ionospheric reflecting layer in field strength calculations at ELF.

## V. Effect of the Earth's Magnetic Field

In the preceding it has been tacitly assumed that the ionosphere is behaving as an isotropic homogeneous conductor. In this case, the refractive index $N_i$ of the ionosphere may be written [23]

$$N_i \cong \left[1 - i\,\frac{\omega_r}{\omega}\right]^{\frac{1}{2}} \cong \left(\frac{\omega_r}{i\omega}\right)^{\frac{1}{2}} \tag{17}$$

where

$$\omega_r = \frac{\omega_o^2}{\nu} = \frac{(\text{Plasma Frequency})^2}{(\text{Collision Frequency})} .$$

When the earth's magnetic field is steeply dipping, it is appropriate to invoke the quasi-longitudinal approximation of Booker [23]. In this case the refractive index is double valued, one corresponds to the ordinary and the other the extra-ordinary, thus

$$N_i \cong \left[1 - i\,\frac{\Omega_r}{\omega}\,\exp(\pm\, i\tau)\right]^{\frac{1}{2}} \tag{18}$$

where

$$\tan\tau = \frac{\omega_L}{\nu} = \frac{\text{longitudinal component of gyro-frequency}}{\text{collision frequency}}$$

and

$$\Omega_r = \frac{\omega_o^2}{(\nu^2 + \omega_L^2)^{\frac{1}{2}}} .$$

Using this model for the ionosphere, the reflection coefficient for a sharp boundary has been derived by Budden [24]. Adapting this result to E.L.F. it has been shown [17] that the formula for $S_n$ has the

same form as the isotropic medium if $\Delta$ is defined by

$$\Delta = \frac{1}{N_g} + \left(\frac{i\omega}{\Omega_r}\right)^{\frac{1}{2}} \cos \tau/2 \quad . \tag{19}$$

Since $\Omega_r = \omega_r \cos \tau$ it is possible to write the results in the same form as the isotropic ionosphere if we set

$$\Delta \cong \frac{1}{N_g} + \frac{1}{(N_i)_{eff.}} \cong \frac{1}{(N_i)_{eff.}}$$

where

$$(N_i)_{eff.} = \left[\frac{(\omega_r)_{eff.}}{i\omega}\right]^{\frac{1}{2}} \quad .$$

$(N_i)_{eff.}$ and $(\omega_r)_{eff.}$ are the effective values of $N_i$ and $\omega_r$, respectively. Specifically,

$$(\omega_r)_{eff.} \cong \omega_r \frac{\cos \tau}{(\cos \tau/2)^2} \quad . \tag{20}$$

In other words, the effective conductivity of the ionosphere is modified by the factor $\frac{\cos \tau}{(\cos \tau/2)^2}$ which varies from unity to zero as $\tau$ varies from 0 to $\pi/2$. Thus, the attenuation is increased as a result of a steeply dipping (or vertical) magnetic field. In fact

$$\frac{\text{Attenuation with magnetic field}}{\text{Attenuation without magnetic field}} \cong \frac{\cos (\tau/2)}{(\cos \tau)^{\frac{1}{2}}} \quad . \tag{21}$$

If $\tau << 1$ (i.e., $\omega_L << \nu$), this ratio becomes unity and the influence of the earth's magnetic field vanishes. At the level in the ionosphere where E.L.F. waves are reflected, it is expected that $\omega_L$ and $\nu$ are comparable, both being of the order of $10^6$. Assuming that they were actually equal, $\tau$ becomes $45^\circ$ and the ratio of the attenuation rates is 1.05. Thus, it is only when $\omega_L$ is greater than $\nu$ does the earth's magnetic field appreciably influence the attenuation. The ratio is plotted in Fig. 9 as a function of tan $\tau$ or $\omega_L/\nu$. This illustrates the situation clearly.

The preceding results are subject to the validity of Booker's quasi-longitudinal approximation of the Appleton-Hartree equation[23].

The validity of this approximation requires that

$$\frac{\omega_T^4}{4\,\omega^2\,\omega_L^2} << \left|\left(1 - \frac{\omega_o^2}{\omega^2} - i\,\frac{\nu}{\omega}\right)^2\right| \tag{22}$$

where $\omega_L$ and $\omega_T$ are the longitudinal and transverse components of the (angular) gyro-frequency. Clearly this condition is violated when the transverse component of the earth's magnetic field is large such as for propagation along the magnetic equator. This case, however, has been considerrd by Barber and Crombie [25] who derived explicit results for the reflection coefficient at a sharply bounded ionosphere with a purely transverse magnetic field. Adapting their results to E. L. F. it is not difficult to show [17] that $\Delta$ is now given by

$$\Delta = \left(\frac{i\omega}{\omega_r}\right)^{\frac{1}{2}} X \tag{23}$$

where

$$X \doteq \frac{\left(1 + \frac{i\omega}{\omega_r}\right)^{\frac{1}{2}}\left(1 + i\,\frac{\omega}{\omega_r} + i\,\frac{\omega_T^2}{\nu^2}\,\frac{\omega}{\omega_r}\right)^{\frac{1}{2}} - \frac{\omega_T}{\nu}\left(i\,\frac{\omega}{\omega_r}\right)^{\frac{1}{2}}}{\left(1 + i\,\frac{\omega}{\omega_r}\right)^2 - \frac{\omega_T^2}{\nu^2}\,\frac{\omega^2}{\omega_r^2}}\,.$$

The real and imaginary parts of $\Delta$ are plotted in Figs. 10a and 10b as a function of the frequency parameter $5 \times 10^5 \times f/\omega_r$ where f is expressed in kc/s and $\omega_r$ is in $(\mathrm{secs})^{-1}$. The various values of $\omega_T/\nu$ are shown in the curves; positive values of the ratio correspond to propagation from east-to-west while negative values correspond to propagation from west-to-east. Now the attenuation of the dominant mode in nepers per unit distances is given by $-kS_o$ where $S_o$ is given by equation (3).

Using the above results for $\Delta$ the attenuation coefficient $\alpha$, expressed in db per 1000 km of path length, is plotted in Fig. 11a for h = 90 km. It is immediately evident that the attenuation is only slightly modified by the presence of a transverse magnetic field unless, of course, $\omega_T$ is considerably greater than $\nu$. The phase velocity of the dominant zero-order mode, relative to free space, is

simply $1/\mathrm{Re}\ S_o$. Denoting this dimensionless quantity by $\beta$ it is plotted in Fig.11b for h = 90 km. It is apparent that the presence of a transverse magnetic field does have an influence on the phase velocity.

## Acknowledgment

We would like to thank John Harman and Barbara Bolton for preparing the illustrations and Eileen Brackett for typing the manuscript.

## References


[1] W.O. Schumann, Uber der ausbreitung sehr langer elektrischer wellen um die erde und die signale des blitze, Il Nuovo Cimento, IX, (1952).

[2] W.O. Schumann, Uber die oberfelder bei der ausbreitung langer, elektrischer wellen im system erde-luft-ionosphare und 2 anwendungen (horizontaler und senkrechter dipol), Zeits fur ange, Phys., 6, 34, (1954).

[3] W.O. Schumann, Uber die strahlung langer wellen des horizontalen dipols in dem lufthohlraum zwischen erde und ionosphare, Seits fur ange Phys., 6, 225, (1954).

[4] J.R. Wait, On the mode theory of VLF ionospheric propagation, Review Geofisica Pura e Applicata, 37, 103, (1957), (paper presented at International URSI Conference of Radio Wave Propagation, Paris, Sept., 1956).

[5] L. Liebermann, Anomalous propagation below 500 c/s, Proc. Sym. on Propagation of VLF Radio Waves, 3, paper no. 25, Boulder, Colorado, (1957).

[6] R.E. Holzer and O.E. Deal, Low audio-frequency electromagnetic signals of natural origin, Nature, 177, 536, (1956).

[7] O.E. Deal, The observation of very low frequency electromagnetic signals of natural origin, unpublished Ph. D. Thesis, The University of California, Los Angeles, 1956.

[8] F.W. Chapman and W.D. Matthews, Audio-frequency spectrum of atmospherics, Nature, 172, 495 (1953).

[9] F. Hepburn and E.T. Pierce, Atmospherics with very low frequency components, Nature, 172, 837, (1953).

[10] H.F. Willis, Audio frequency magnetic fluctuations, Nature, 161, 887, (1948).

[11] J. Aarons and M. Henissart, Low frequency noise in the range 0.5 to 20 c/s, Nature, 172, 682, (1953).

[12] R. Beniot, Low frequency radio wave noise of the earth's magnetic field, C. R. Acad. Sci., 242, 2534, (1956).

[13] P.A. Goldberg, Electromagnetic phenomena of natural origin in the 1.0 - 150 c/s band, Nature, 177, 1219, (1956).

[14] J. Aarons, Low frequency electromagnetic radiation 10 to 900 c/s, J. Geophs. Res., 61, 647, (1956).

[15] J.M. Watts, An observation of audio-frequency electromagnetic noise during a period of solar disturbance, J. Geophs. Res., 62, 199, (1957).

[16] J.R. Wait, An extension to the mode theory of VLF ionospheric region, Jour. Geophys. Res., 63, 125, (1958).

[17] J.R. Wait, Terrestrial propagation of VLF radio waves, J. Research NBS, 64D, 153, (1960).

[18] H. Motz, Electromagnetic problems of microwave theory, Methuen and Company, 1951.

[19] H.R.L. Lamont, Waveguides, Methuen and Company, 1942.

[20] C.L. Pekeris, Accuracy of the earth-flattening approximation in the theory of microwave propagation, Phys. Rev., 70, 518, (1946).

[21] B.Y.-C. Koo and M. Katzin, An exact earth-flattening procedure in propagation around a sphere, J. Research NBS, 64D, 61, (1960).

[22] J.R. Wait, The mode theory of VLF ionospheric propagation for finite ground conductivity, Proc. IRE, 45, 760, (1957).

[23] J.A. Ratcliffe, Magneto-ionic theory, Cambridge Univ. Press, 1959.

[24] K.G. Budden, The reflection of very low frequency radio waves at the surface of a sharply bounded ionosphere with superimposed magnetic field, Phil. Mag., 42, 504, (1951).

[25] N.F. Barber and D. D. Crombie, V.L.F. reflections from the ionosphere in the presence of a transverse magnetic field, Jour. Atmos. Terr. Phys., 16, 37, (1959).

[26] J. R. Wait and H. H. Howe, Amplitude and phase for ground wave propagation in the band 200 c/s to 500 kc, NBS Circular 574, 1956.

## Figure Captions

Figs. 1a, b, c, The normalized magnitude of the magnetic field as a function of distance from the source ($\rho$ is expressed in kilometers in both ordinate and abscissa).

Figs. 2a, b, c, The normalized phase (lag), in radians, of the magnetic field.

Figs. 3a, b, c, The normalized magnitude of the electric field as a function of distance from the source.

Figs. 4a, b, c, The normalized phase (lag) of the electric field.

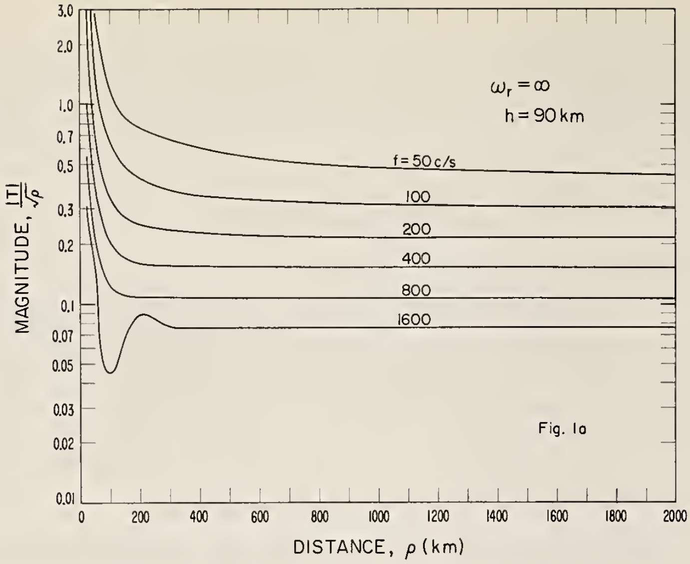


Fig. 1a

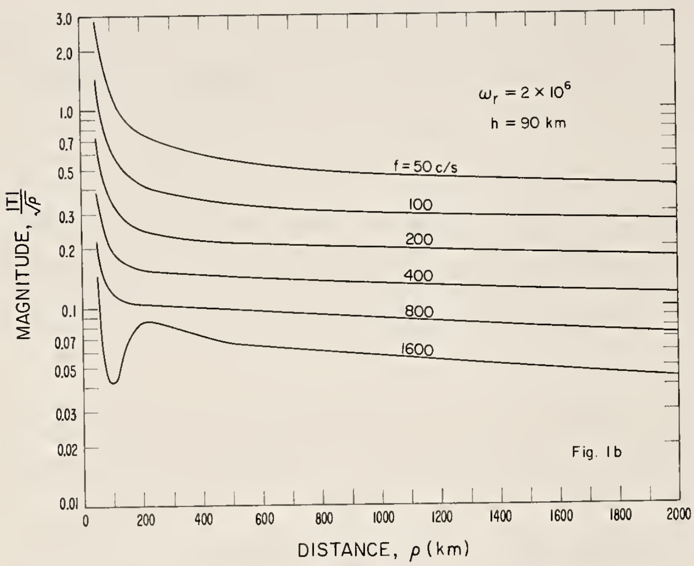


Fig. 1b

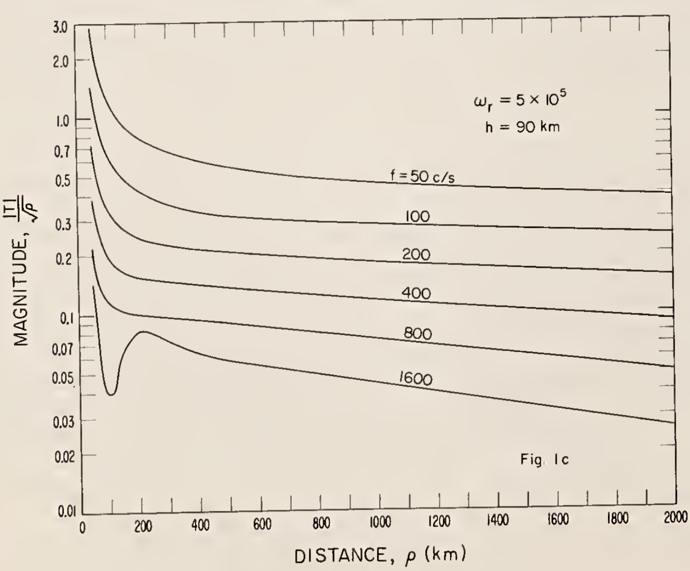


Fig. 1c

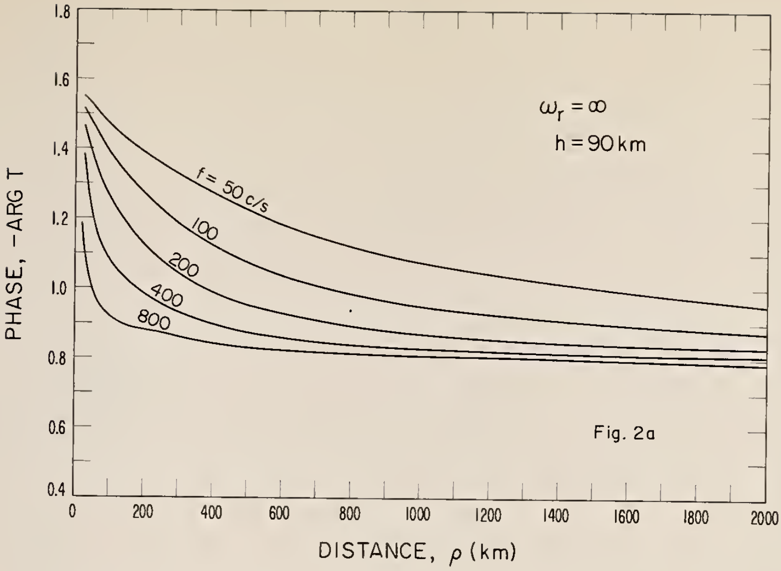


Fig. 2a

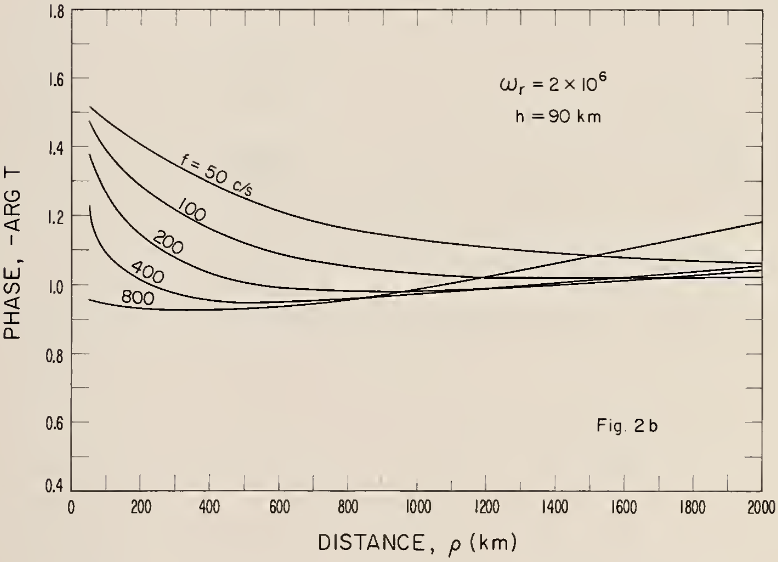


Fig. 2b

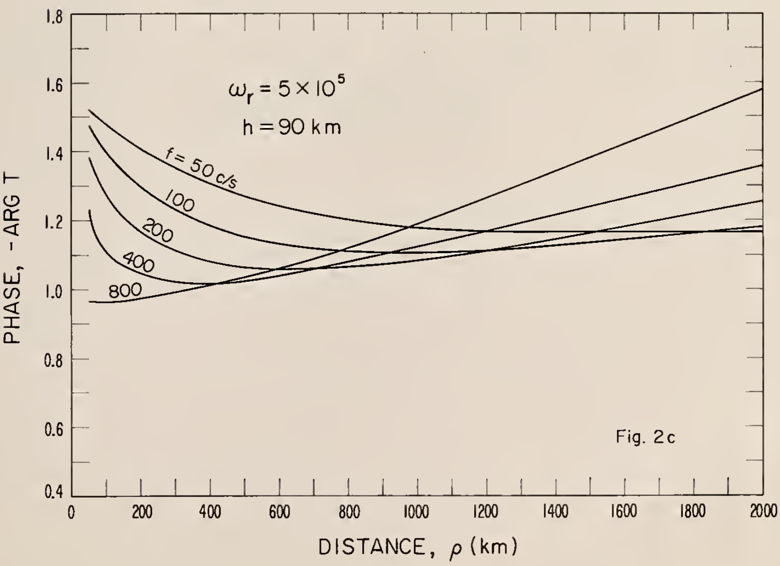


Fig. 2c

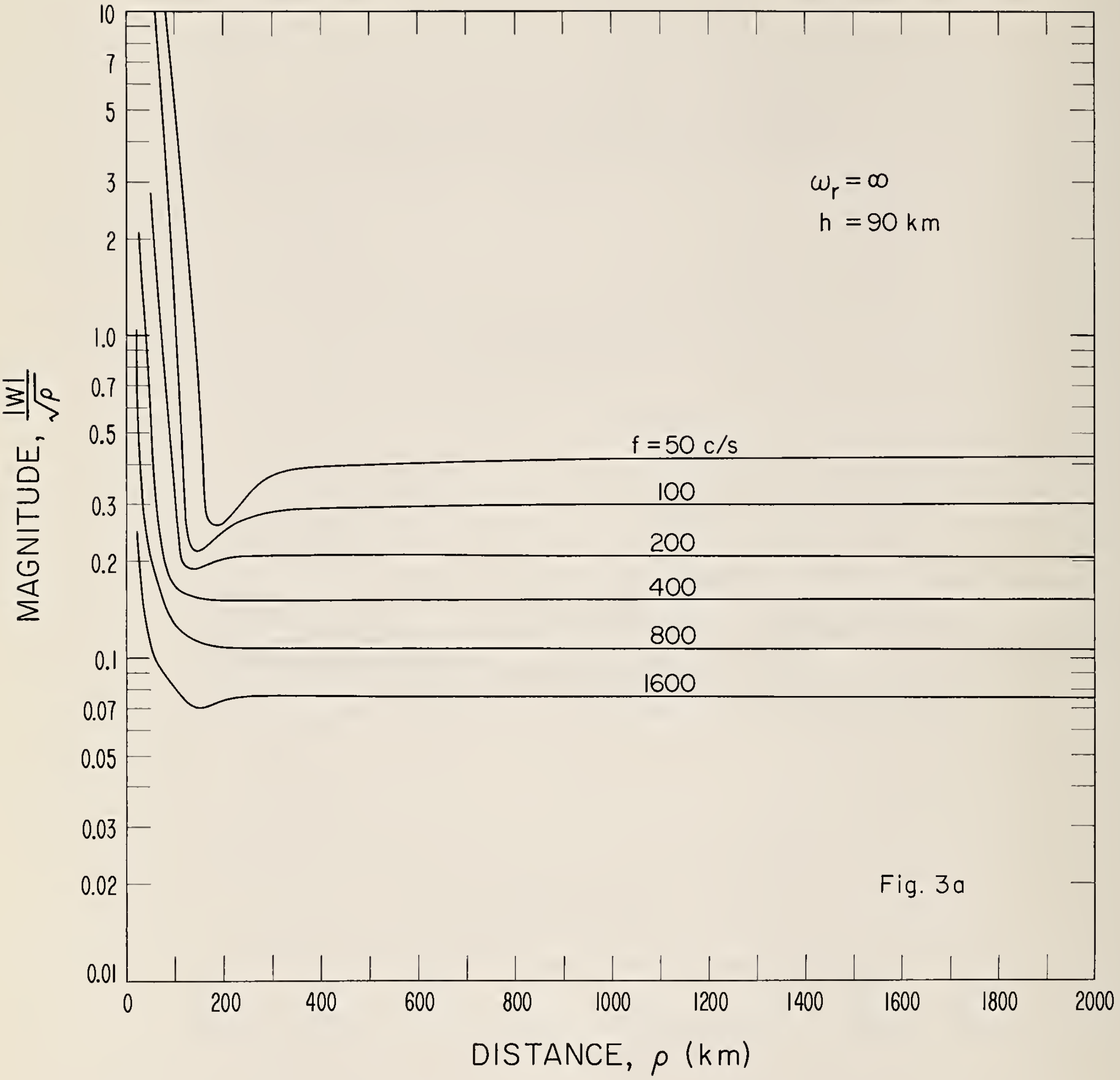

$\omega_r = \infty$
h = 90 km
f = 50 c/s
100
200
400
800
1600
MAGNITUDE, $\frac{|W|}{\sqrt{\rho}}$
DISTANCE, $\rho$ (km)
10
7
5
3
2
1.0
0.7
0.5
0.3
0.2
0.1
0.07
0.05
0.03
0.02
0.01
0
200
400
600
800
1000
1200
1400
1600
1800
2000


Fig. 3a

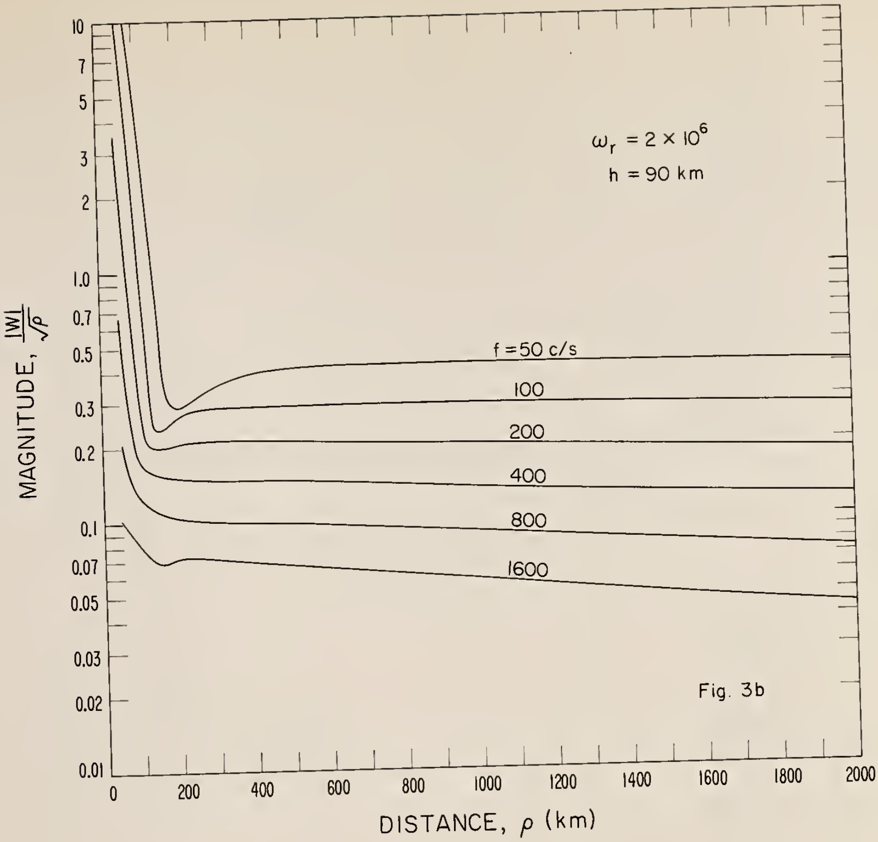
$\omega_r = 2 \times 10^6$
h = 90 km
f = 50 c/s
100
200
400
800
1600
MAGNITUDE, $\frac{|W|}{\sqrt{\rho}}$
DISTANCE, $\rho$ (km)
10
7
5
3
2
1.0
0.7
0.5
0.3
0.2
0.1
0.07
0.05
0.03
0.02
0.01
0
200
400
600
800
1000
1200
1400
1600
1800
2000

Fig. 3b

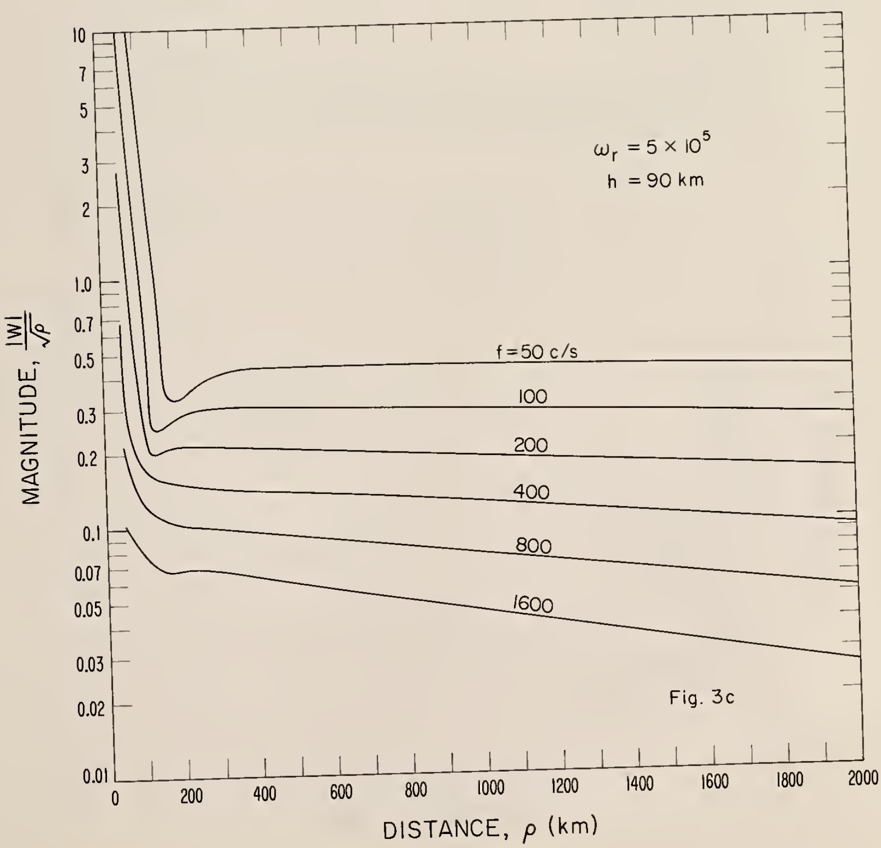
$\omega_r = 5 \times 10^5$
h = 90 km
f = 50 c/s
100
200
400
800
1600
MAGNITUDE, $\frac{|W|}{\sqrt{\rho}}$
DISTANCE, $\rho$ (km)
10
7
5
3
2
1.0
0.7
0.5
0.3
0.2
0.1
0.07
0.05
0.03
0.02
0.01
0
200
400
600
800
1000
1200
1400
1600
1800
2000

Fig. 3c

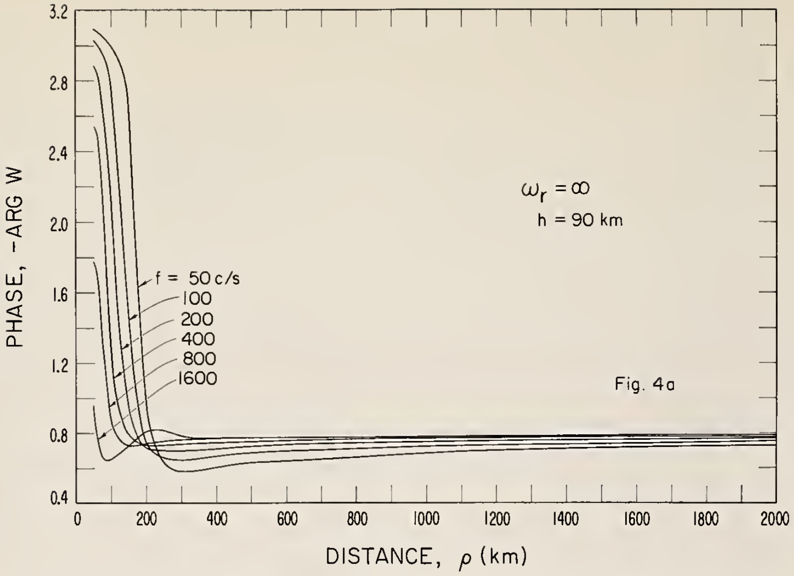
PHASE, −ARG W
DISTANCE, ρ (km)
ω_r = ∞
h = 90 km
f = 50 c/s
100
200
400
800
1600
Fig. 4a

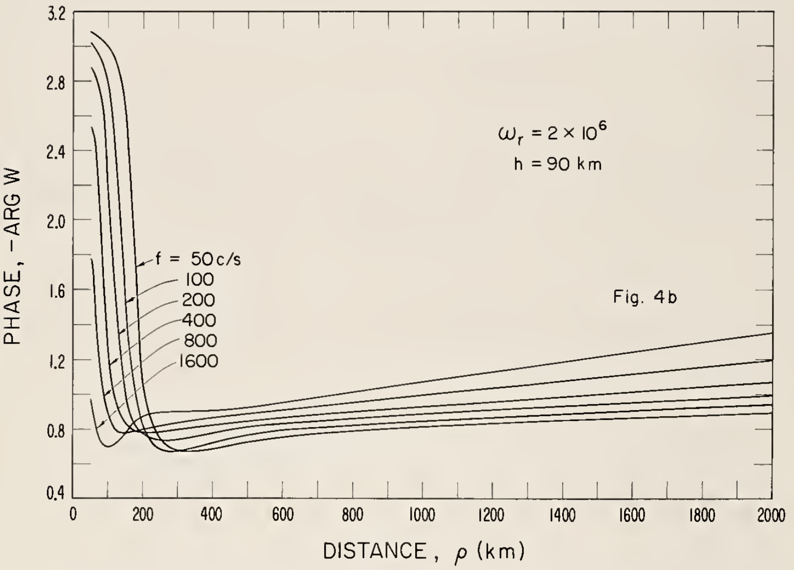
PHASE, −ARG W
DISTANCE, ρ (km)
ω_r = 2 × 10^6
h = 90 km
f = 50 c/s
100
200
400
800
1600
Fig. 4b

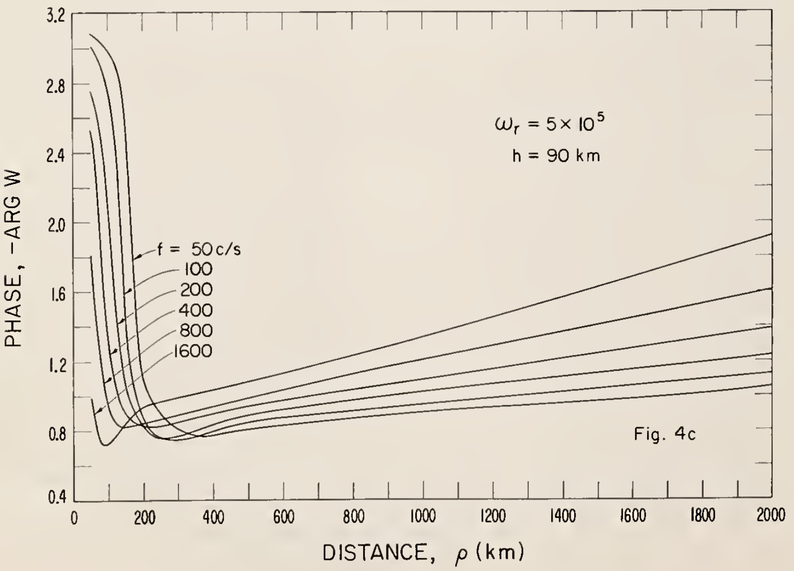
PHASE, −ARG W
DISTANCE, ρ (km)
ω_r = 5 × 10^5
h = 90 km
f = 50 c/s
100
200
400
800
1600
Fig. 4c

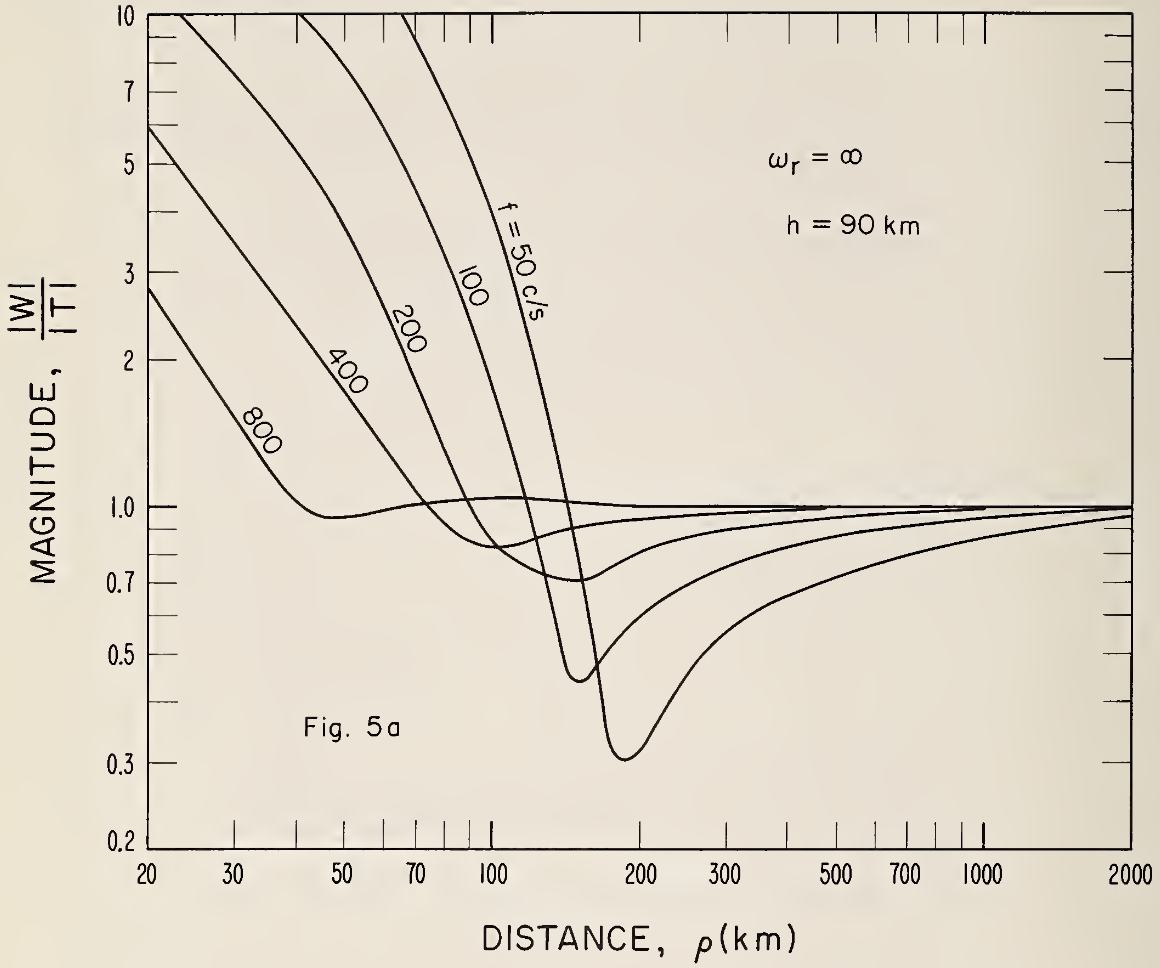

$\omega_r = \infty$
$h = 90$ km
$f = 50$ c/s
100
200
400
800
MAGNITUDE, $\frac{|W|}{|T|}$
DISTANCE, $\rho$(km)
10
7
5
3
2
1.0
0.7
0.5
0.3
0.2
20
30
50
70
100
200
300
500
700
1000
2000

Fig. 5a

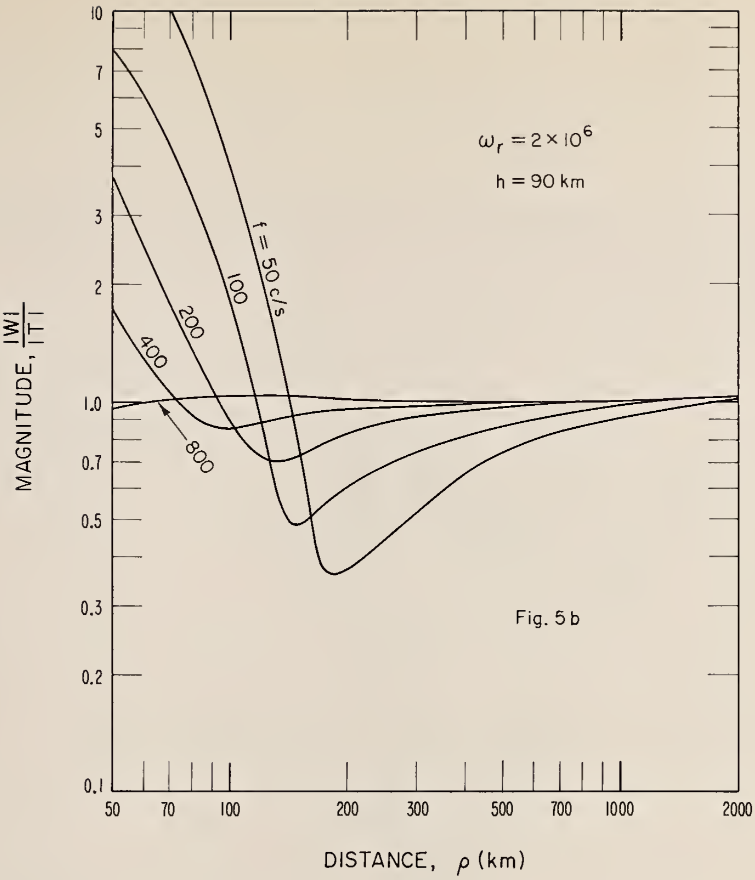
$\omega_r = 2 \times 10^6$
h = 90 km
f = 50 c/s
100
200
400
800
MAGNITUDE, $\frac{|W|}{|T|}$
DISTANCE, $\rho$ (km)
Fig. 5 b

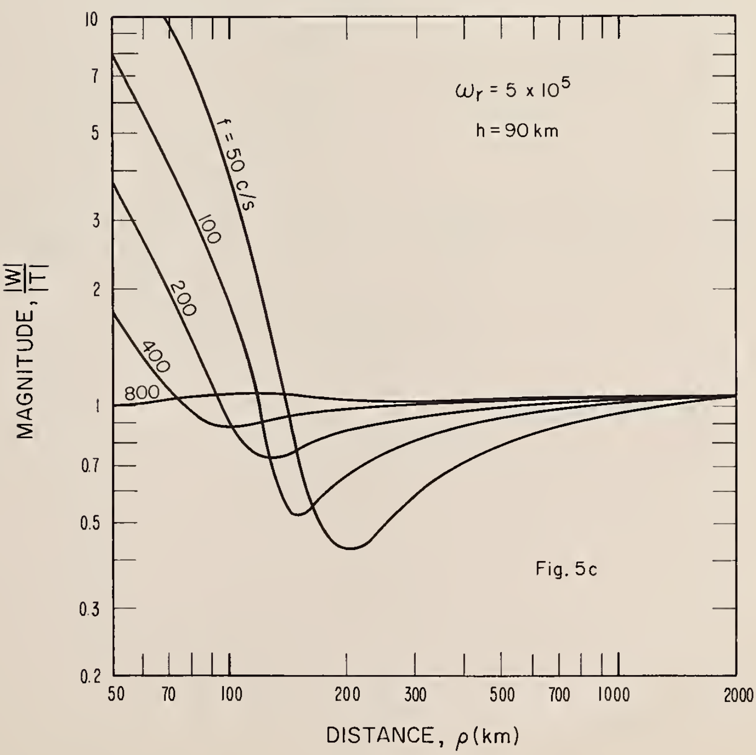
$\omega_r = 5 \times 10^5$
h = 90 km
f = 50 c/s
100
200
400
800
MAGNITUDE, $\frac{|W|}{|T|}$
DISTANCE, $\rho$ (km)
Fig. 5c

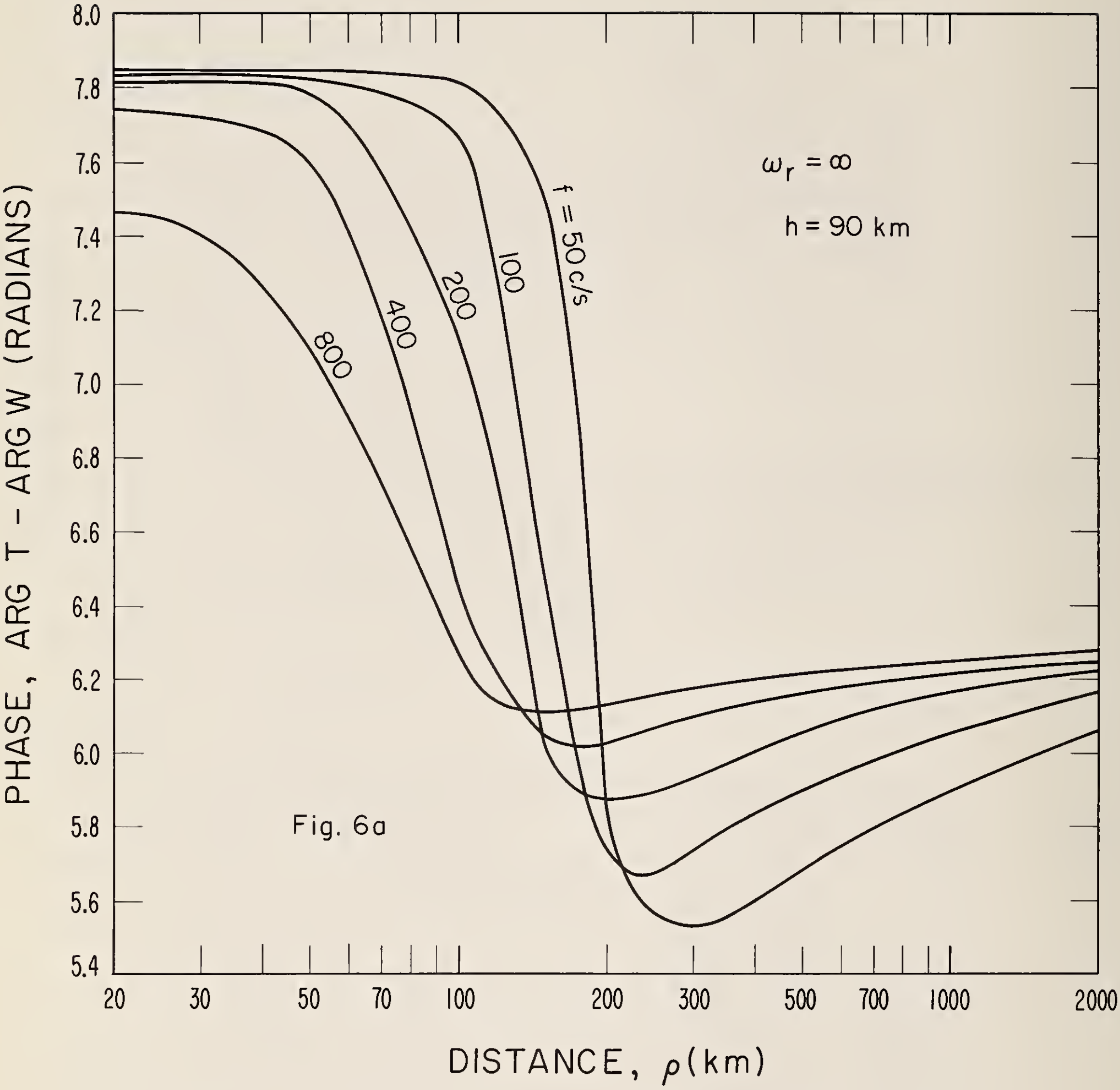
PHASE, ARG T - ARG W (RADIANS)
8.0
7.8
7.6
7.4
7.2
7.0
6.8
6.6
6.4
6.2
6.0
5.8
5.6
5.4
20
30
50
70
100
200
300
500
700
1000
2000
DISTANCE, $\rho$(km)
$\omega_r = \infty$
h = 90 km
f = 50c/s
100
200
400
800

Fig. 6a

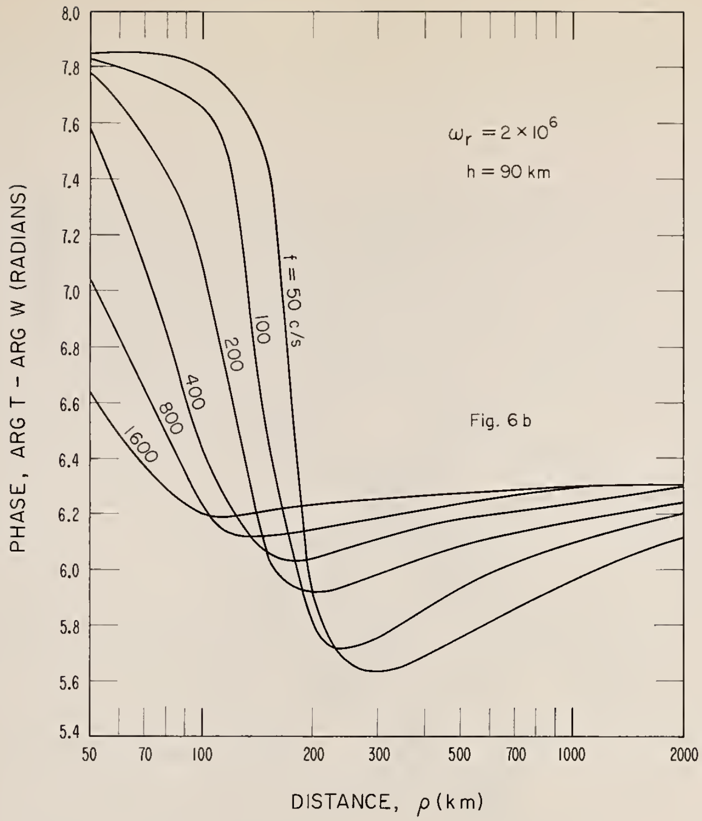

$\omega_r = 2 \times 10^6$
h = 90 km
f = 50 c/s
100
200
400
800
1600
PHASE, ARG T - ARG W (RADIANS)
DISTANCE, $\rho$ (km)


Fig. 6 b

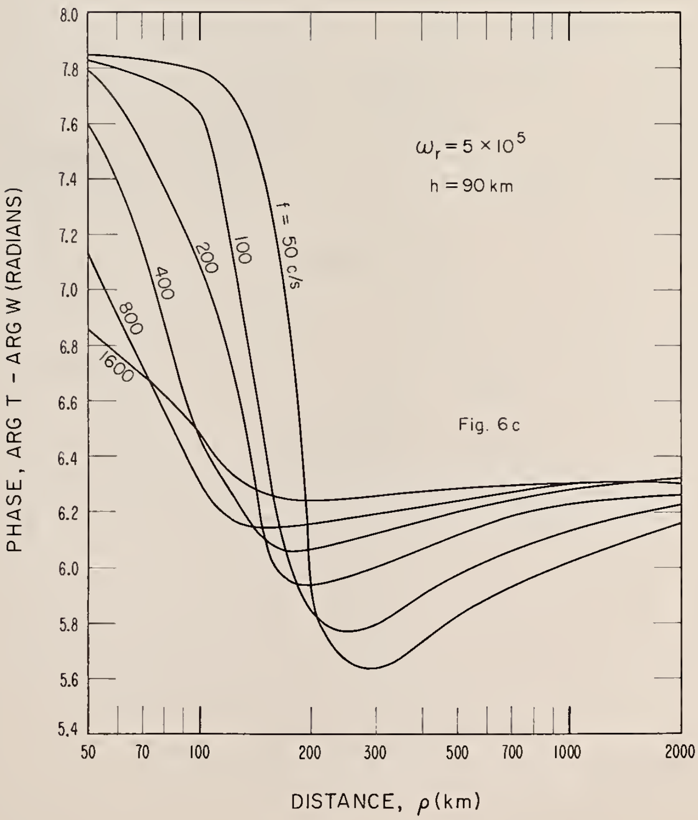

$\omega_r = 5 \times 10^5$
h = 90 km
f = 50 c/s
100
200
400
800
1600
PHASE, ARG T - ARG W (RADIANS)
DISTANCE, $\rho$ (km)


Fig. 6 c

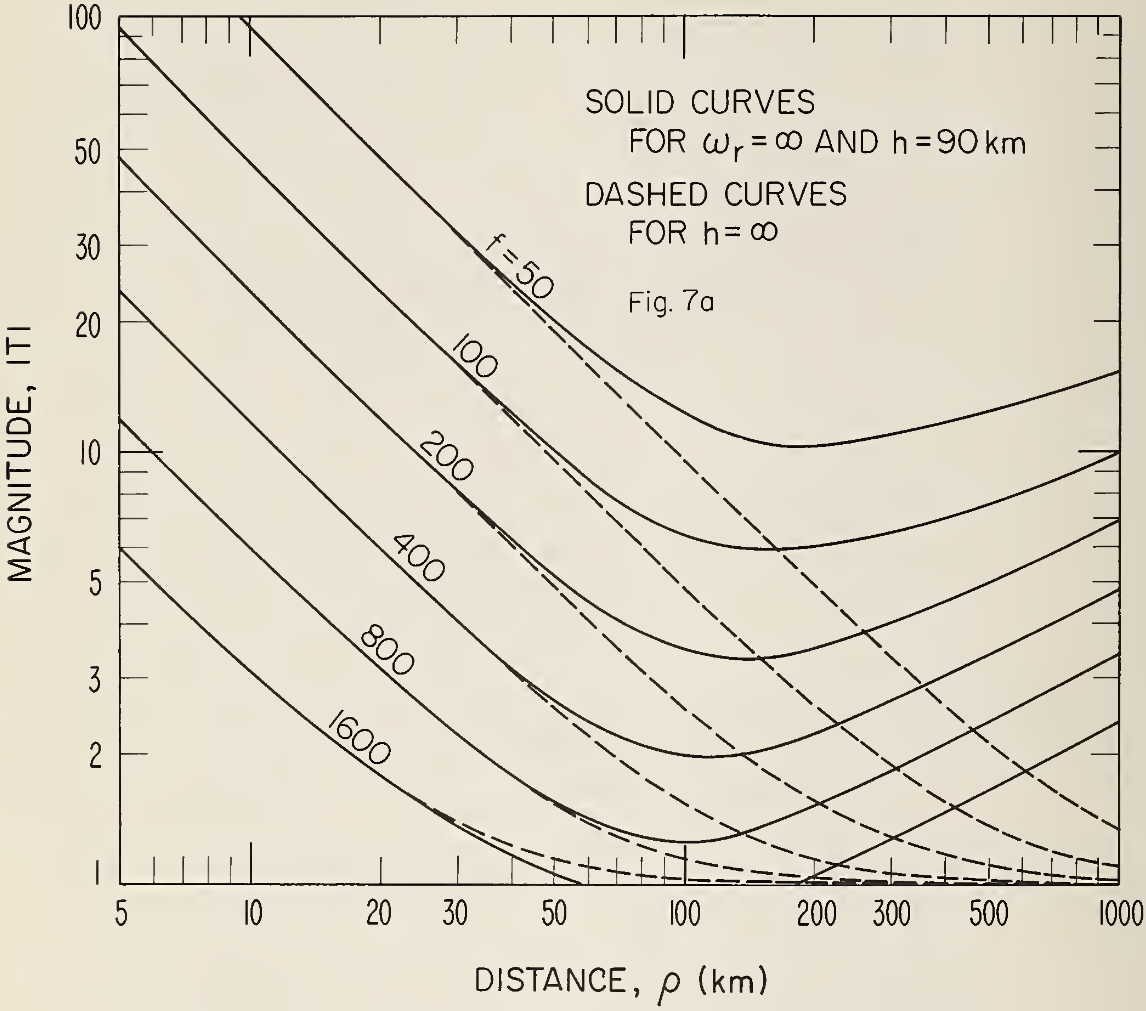
SOLID CURVES
FOR $\omega_r = \infty$ AND h = 90 km
DASHED CURVES
FOR $h = \infty$
Fig. 7a
f = 50
100
200
400
800
1600
MAGNITUDE, |T|
DISTANCE, $\rho$ (km)
100
50
30
20
10
5
3
2
1
5
10
20
30
50
100
200
300
500
1000

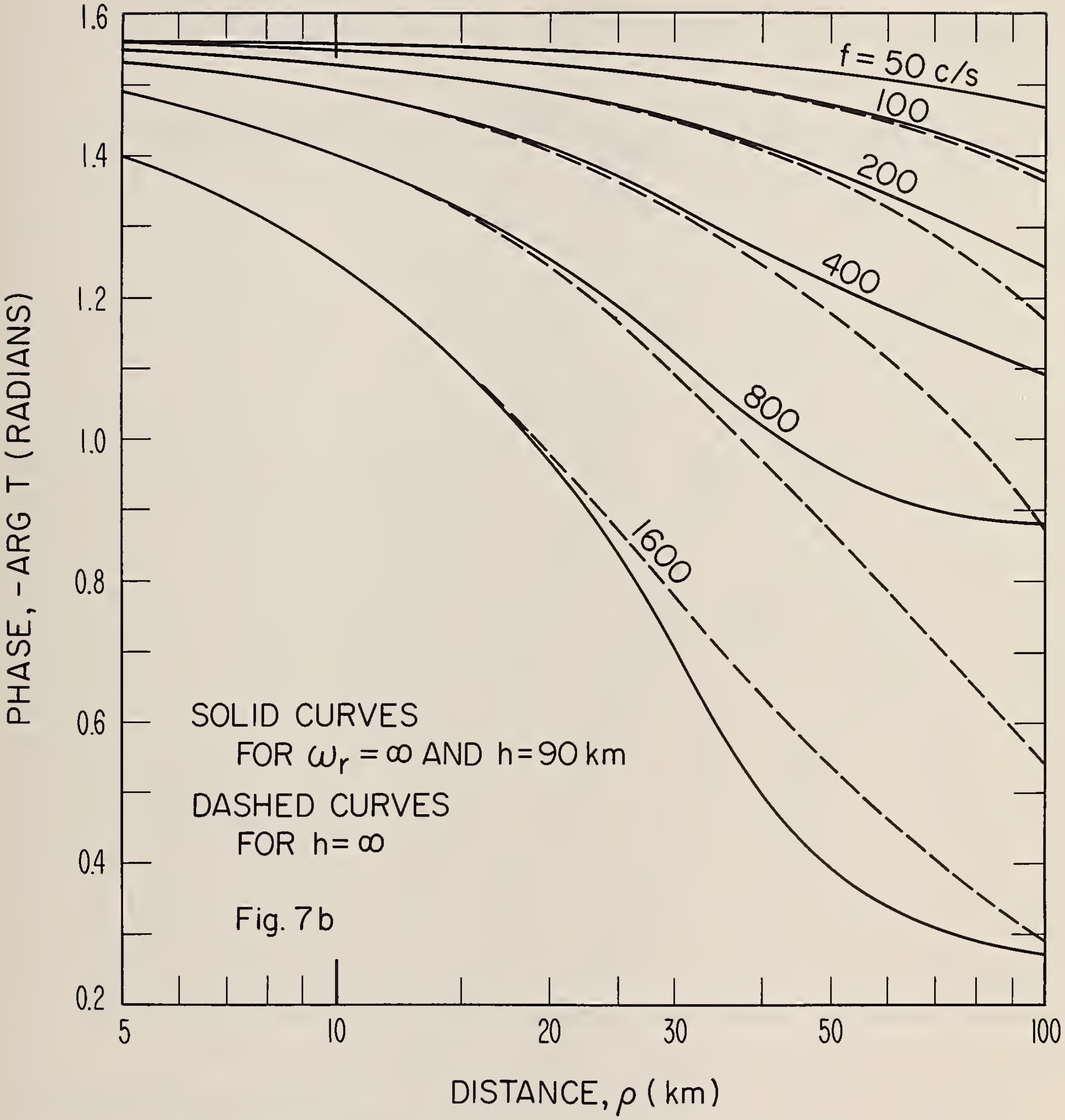

1.6
1.4
1.2
1.0
0.8
0.6
0.4
0.2
PHASE, -ARG T (RADIANS)
f = 50 c/s
100
200
400
800
1600
SOLID CURVES
FOR $\omega_r = \infty$ AND h = 90 km
DASHED CURVES
FOR h = $\infty$
5
10
20
30
50
100
DISTANCE, $\rho$ (km)


Fig. 7b

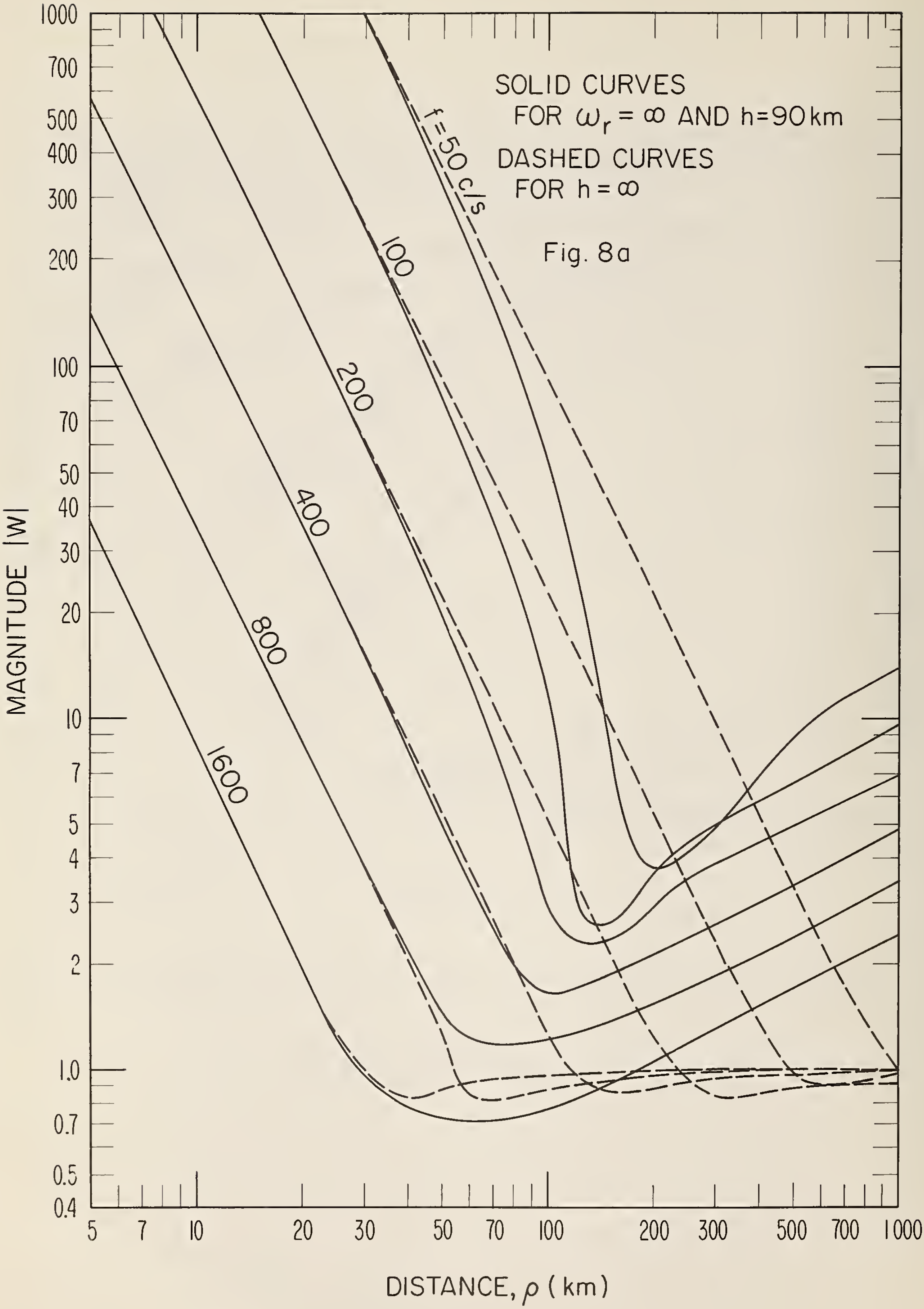

SOLID CURVES
FOR $\omega_r = \infty$ AND h=90 km
DASHED CURVES
FOR $h = \infty$
f=50 c/s
100
200
400
800
1600
MAGNITUDE |W|
1000
700
500
400
300
200
100
70
50
40
30
20
10
7
5
4
3
2
1.0
0.7
0.5
0.4
5
7
10
20
30
50
70
100
200
300
500
700
1000
DISTANCE, $\rho$ (km)

Fig. 8a

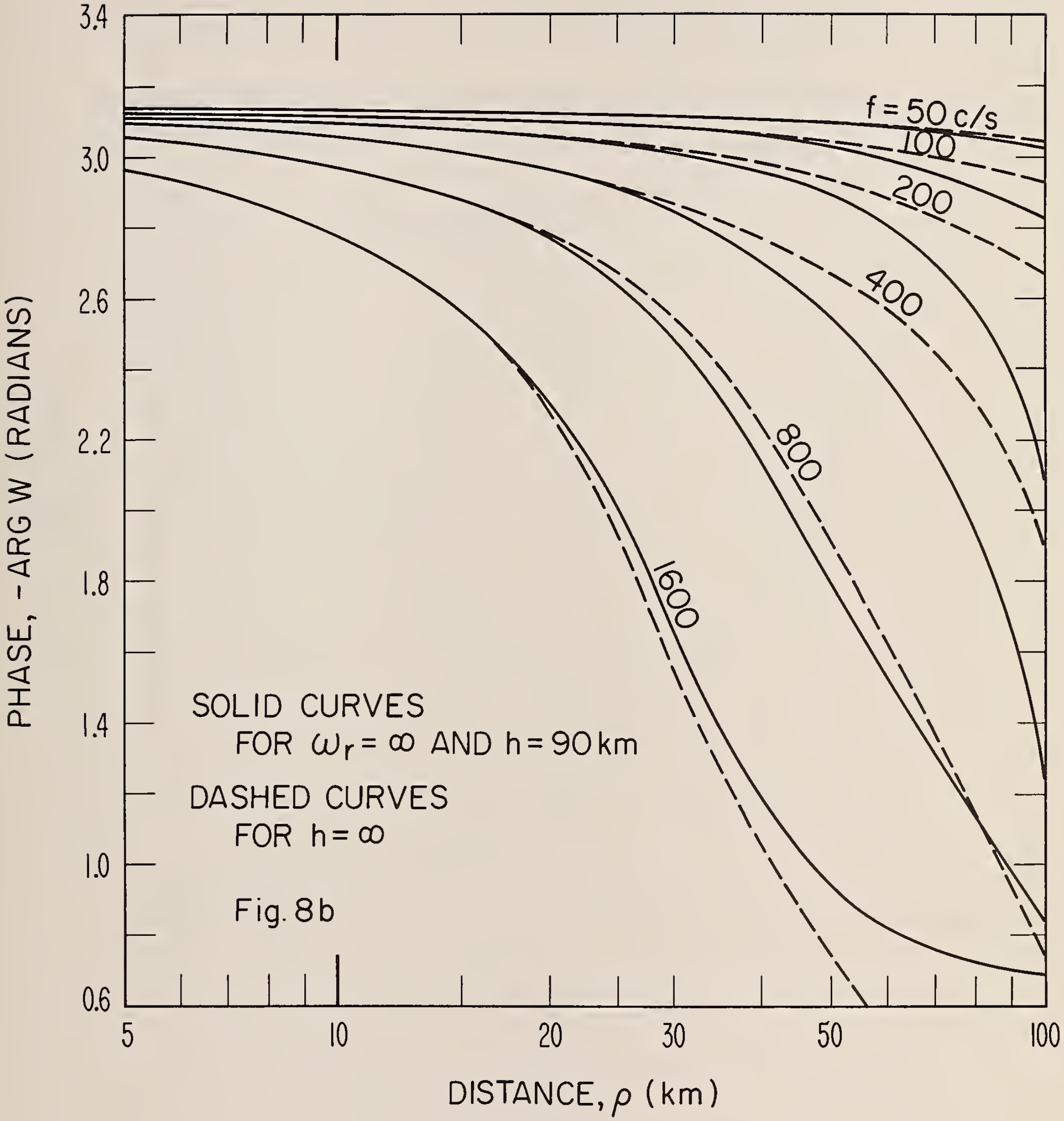

3.4
3.0
2.6
2.2
1.8
1.4
1.0
0.6
PHASE, - ARG W (RADIANS)
5
10
20
30
50
100
DISTANCE, $\rho$ (km)
f = 50 c/s
100
200
400
800
1600
SOLID CURVES
FOR $\omega_r = \infty$ AND h = 90 km
DASHED CURVES
FOR h = $\infty$


Fig. 8b

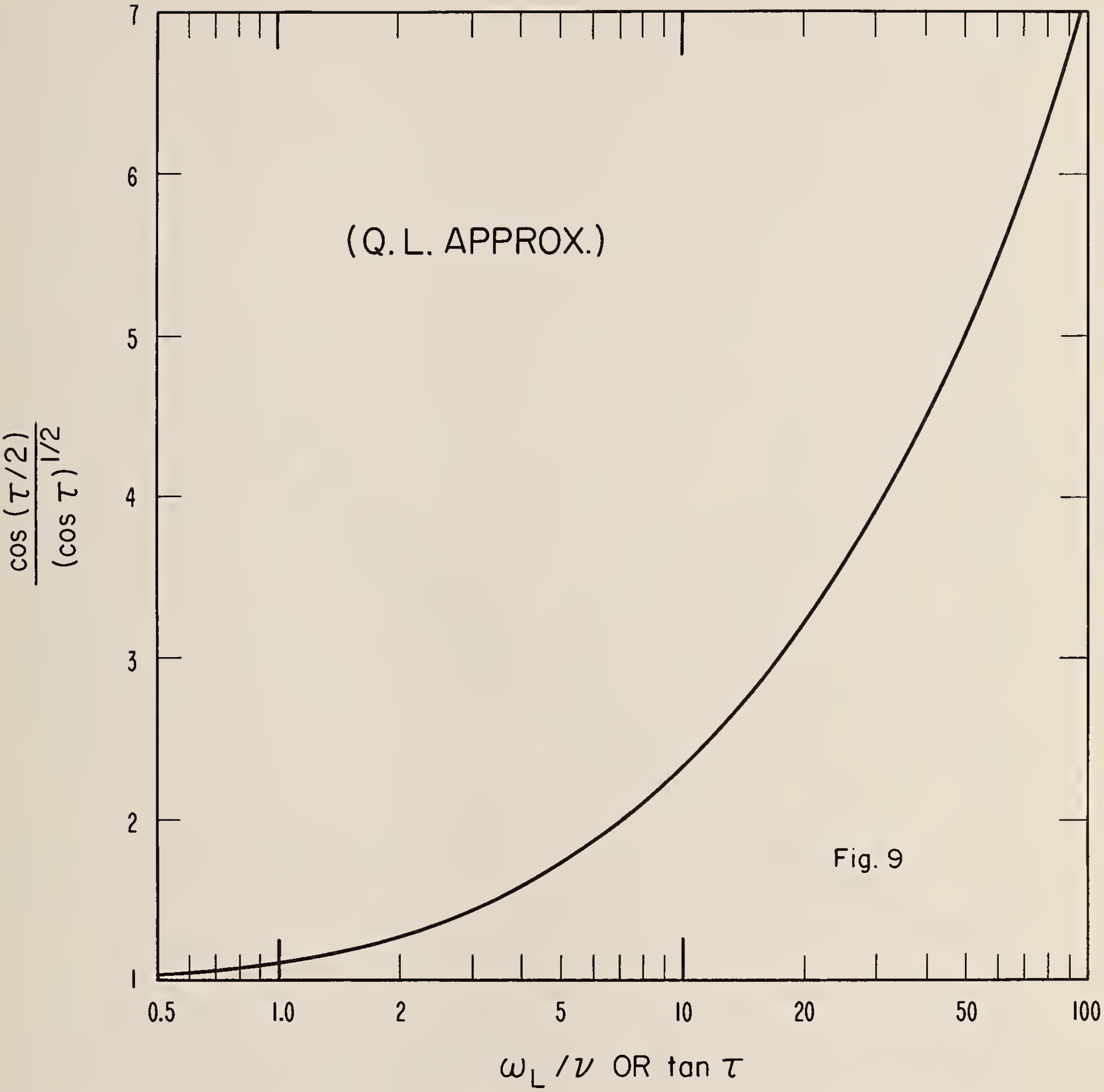
(Q. L. APPROX.)
$\frac{\cos(\tau/2)}{(\cos\tau)^{1/2}}$
1
2
3
4
5
6
7
0.5
1.0
2
5
10
20
50
100
$\omega_L/\nu$ OR $\tan\tau$

Fig. 9

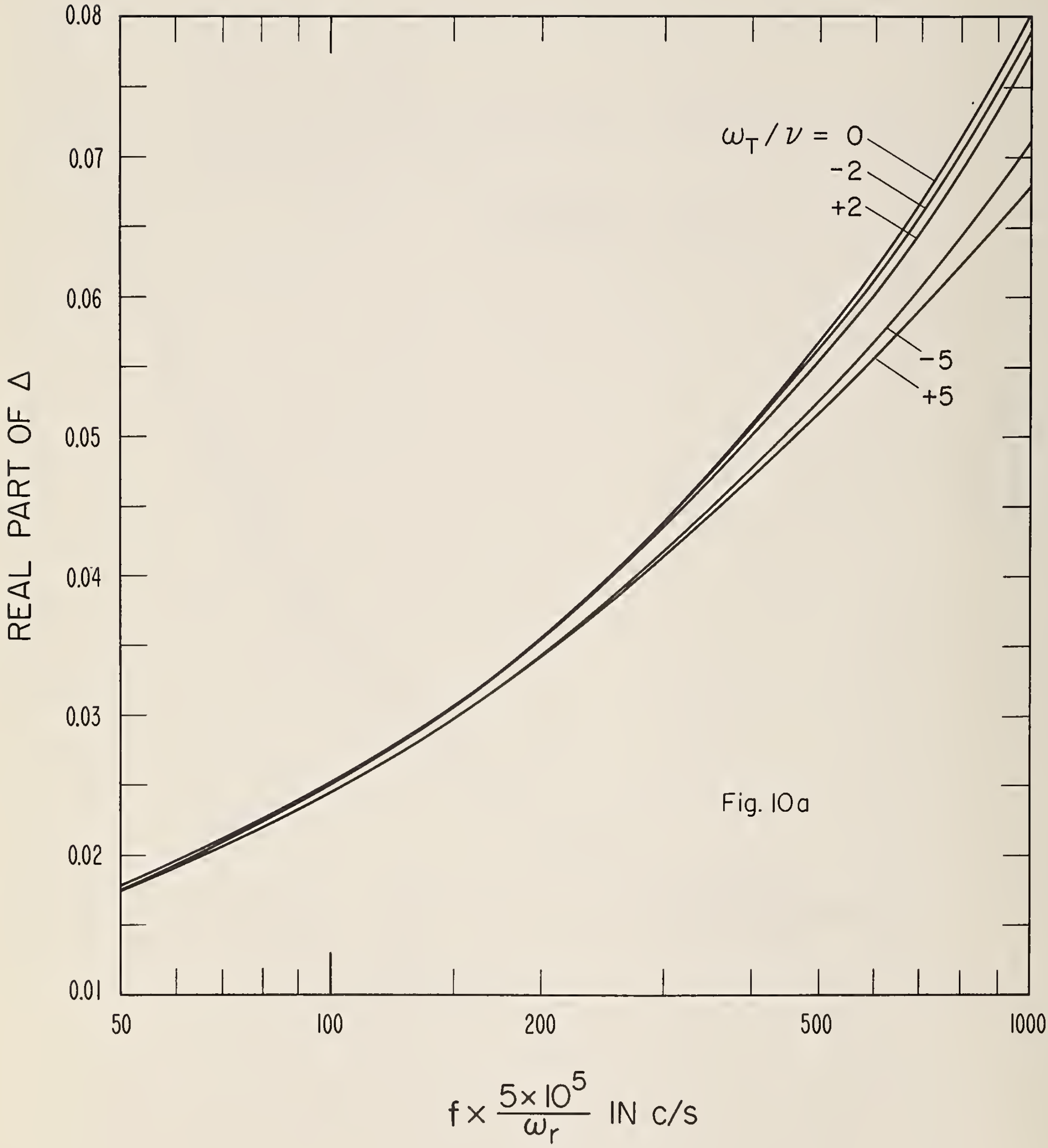
0.08
0.07
0.06
0.05
0.04
0.03
0.02
0.01
REAL PART OF $\Delta$
$\omega_T / \nu = 0$
-2
+2
-5
+5
50
100
200
500
1000
$f \times \frac{5 \times 10^5}{\omega_r}$ IN c/s

Fig. 10a

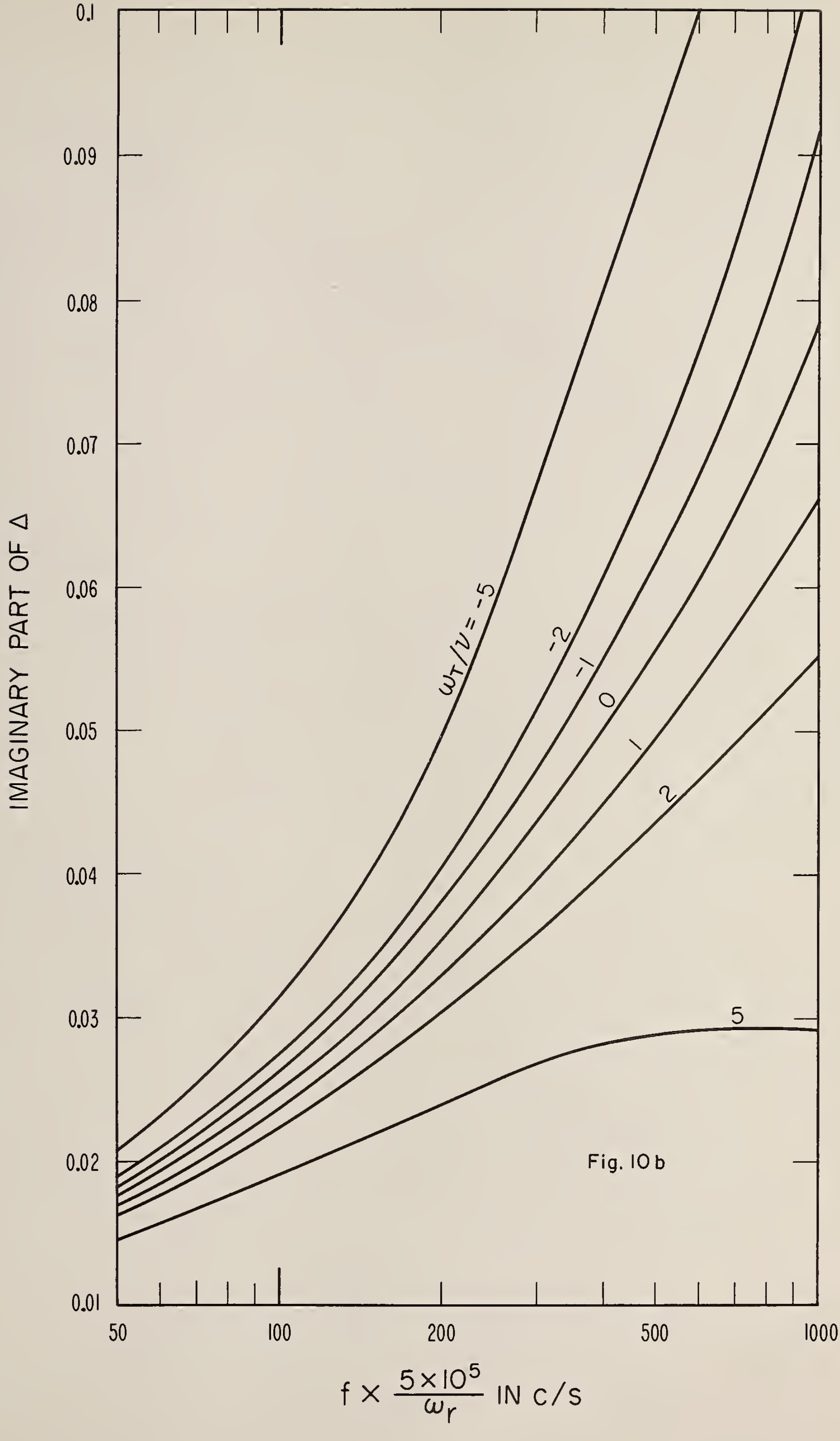
IMAGINARY PART OF Δ
0.1
0.09
0.08
0.07
0.06
0.05
0.04
0.03
0.02
0.01
50
100
200
500
1000
$f \times \frac{5\times10^5}{\omega_r}$ IN c/s
$\omega_T/\nu = -5$
-2
-1
0
1
2
5

Fig. 10 b

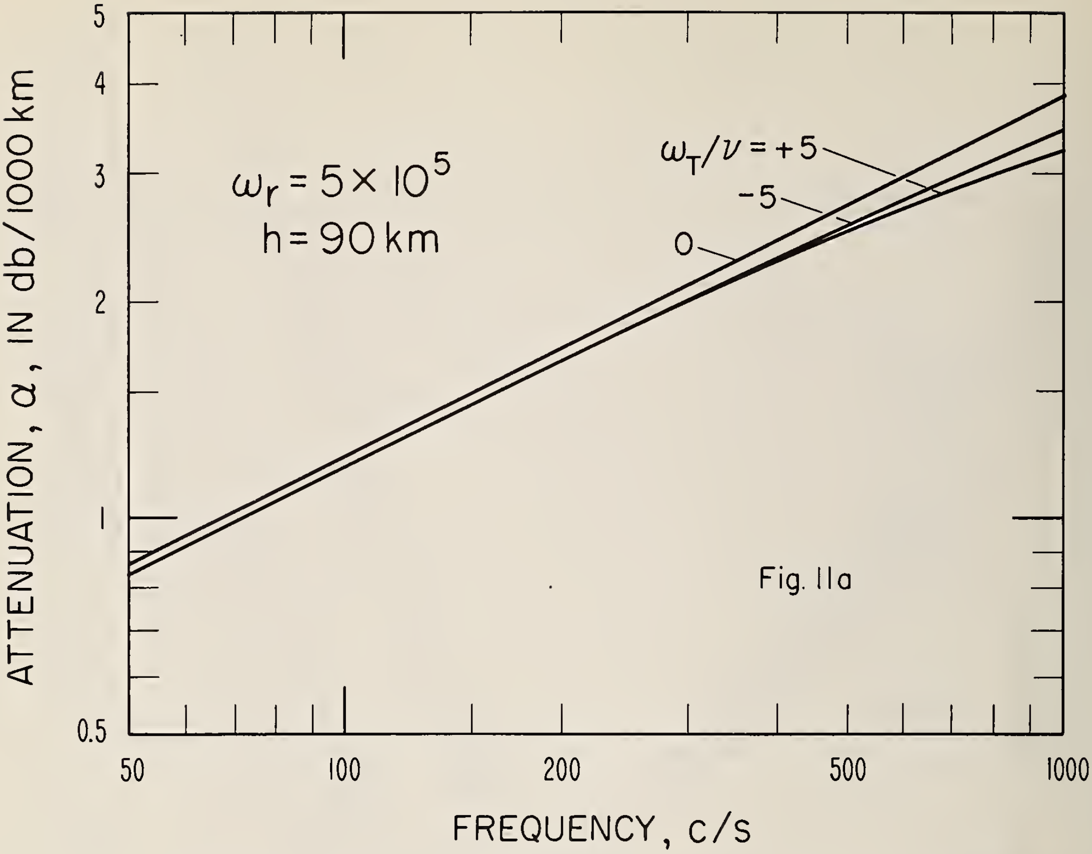


Fig. 11a

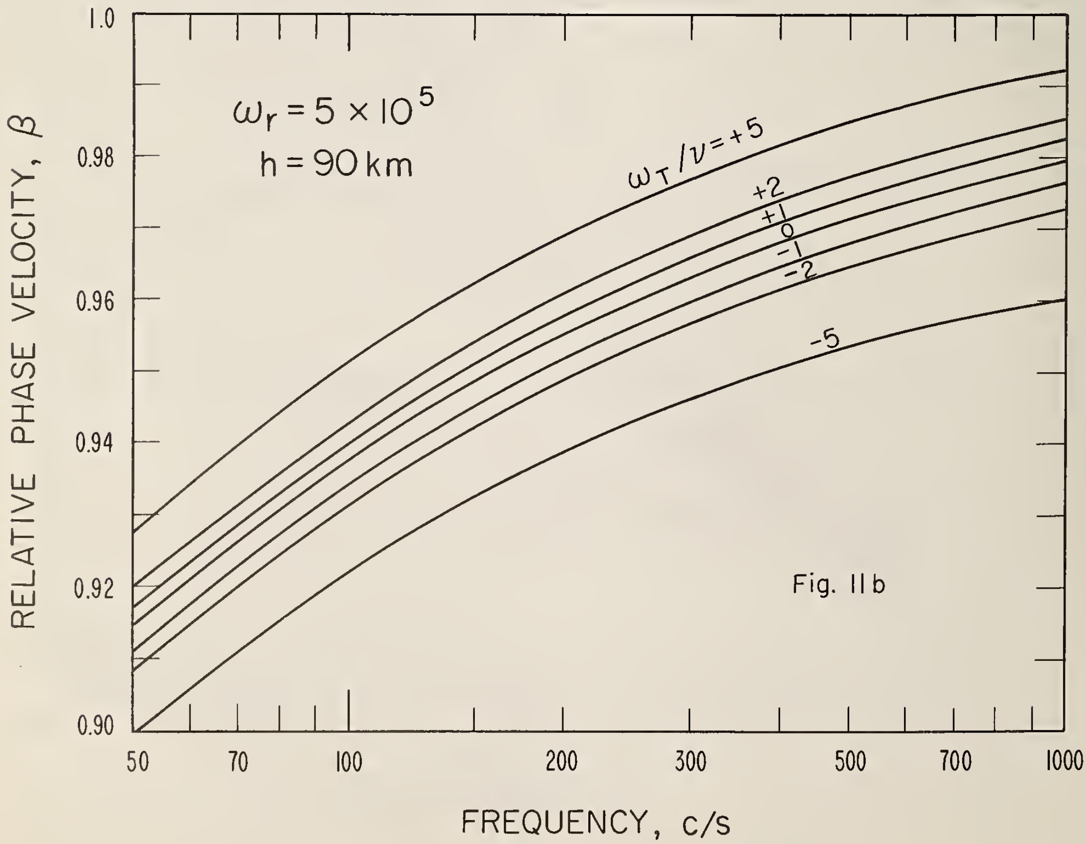


Fig. 11b

U.S. DEPARTMENT OF COMMERCE
Frederick H. Mueller, *Secretary*

NATIONAL BUREAU OF STANDARDS
A. V. Astin, *Director*

# THE NATIONAL BUREAU OF STANDARDS

The scope of activities of the National Bureau of Standards at its major laboratories in Washington, D.C., and Boulder, Colorado, is suggested in the following listing of the divisions and sections engaged in technical work. In general, each section carries out specialized research, development, and engineering in the field indicated by its title. A brief description of the activities, and of the resultant publications, appears on the inside of the front cover.

## WASHINGTON, D.C.

**Electricity and Electronics.** Resistance and Reactance. Electron Devices. Electrical Instruments. Magnetic Measurements. Dielectrics. Engineering Electronics. Electronic Instrumentation. Electrochemistry.

**Optics and Metrology.** Photometry and Colorimetry. Photographic Technology. Length. Engineering Metrology.

**Heat.** Temperature Physics. Thermodynamics. Cryogenic Physics. Rheology. Molecular Kinetics. Free Radicals Research.

**Atomic and Radiation Physics.** Spectroscopy. Radiometry. Mass Spectrometry. Solid State Physics. Electron Physics. Atomic Physics. Neutron Physics. Radiation Theory. Radioactivity. X-rays. High Energy Radiation. Nucleonic Instrumentation. Radiological Equipment.

**Chemistry.** Organic Coatings. Surface Chemistry. Organic Chemistry. Analytical Chemistry. Inorganic Chemistry. Electrodeposition. Molecular Structure and Properties of Gases. Physical Chemistry. Thermochemistry. Spectrochemistry. Pure Substances.

**Mechanics.** Sound. Mechanical Instruments. Fluid Mechanics. Engineering Mechanics. Mass and Scale. Capacity, Density, and Fluid Meters. Combustion Controls.

**Organic and Fibrous Materials.** Rubber. Textiles. Paper. Leather. Testing and Specifications. Polymer Structure. Plastics. Dental Research.

**Metallurgy.** Thermal Metallurgy. Chemical Metallurgy. Mechanical Metallurgy. Corrosion. Metal Physics.

**Mineral Products.** Engineering Ceramics. Glass. Refractories. Enameled Metals. Constitution and Microstructure.

**Building Technology.** Structural Engineering. Fire Protection. Air Conditioning, Heating, and Refrigeration. Floor, Roof, and Wall Coverings. Codes and Safety Standards. Heat Transfer. Concreting Materials.

**Applied Mathematics.** Numerical Analysis. Computation. Statistical Engineering. Mathematical Physics.

**Data Processing Systems.** SEAC Engineering Group. Components and Techniques. Digital Circuitry. Digital Systems. Analog Systems. Application Engineering.

• Office of Basic Instrumentation.

• Office of Weights and Measures.

## BOULDER, COLORADO

**Cryogenic Engineering.** Cryogenic Equipment. Cryogenic Processes. Properties of Materials. Gas Liquefaction.

**Radio Propagation Physics.** Upper Atmosphere Research. Ionospheric Research. Regular Propagation Services. Sun-Earth Relationships. VHF Research. Radio Warning Services. Airglow and Aurora. Radio Astronomy and Arctic Propagation.

**Radio Propagation Engineering.** Data Reduction Instrumentation. Modulation Research. Radio Noise. Tropospheric Measurements. Tropospheric Analysis. Propagation Obstacles Engineering. Radio-Meteorology. Lower Atmosphere Physics.

**Radio Standards.** High Frequency Electrical Standards. Radio Broadcast Service. High Frequency Impedance Standards. Electronic Calibration Center. Microwave Physics. Microwave Circuit Standards.

**Radio Communication and Systems.** Low Frequency and Very Low Frequency Research. High Frequency and Very High Frequency Research. Ultra High Frequency and Super High Frequency Research. Modulation Research. Antenna Research. Navigation Systems. Systems Analysis. Field Operations.

NBS